LOSS OF DJ-1 PROTEIN LEADS TO TISSUE SPECIFIC ACCUMULATION OF ADVANCED GLYCATION END PRODUCTS

NATALIA PRUDENTE DE MELLO

Graduate School of Systemic Neurosciences

LMU Munich

Dissertation at the
Graduate School of Systemic Neurosciences
Ludwig-Maximilians-Universität München

May 2024

Supervisor
Prof. Dr. Fabiana Perocchi
Institute of Neuronal Cell Biology, Technical University of Munich
Institute for Diabetes and Obesity, Helmholtz Zentrum Munich

First Reviewer: Prof. Dr. Fabiana Perocchi
Second Reviewer: Prof. Dr. Mikael Simons
Third Reviewer: Dr. Stefanie Hauck
External Reviewer: Prof. Dr. Cristina Mammucari

Date of Submission: May 10, 2024
Date of Defense: May 06, 2025

Table of Contents

ABSTRACT

It is well known that the multifunctional DJ-1 protein plays an important role in the antioxidative system, a common denominator for several diseases, from metabolic syndrome (MetS) to neurodegenerative diseases such as Parkinson's disease (PD). Among several described functions, DJ-1 was proposed to act as a deglycase, avoiding the accumulation of advanced glycation end products (AGEs), which are known to be involved in diabetes complications, cancer, and neurodegenerative diseases. However, the deglycase activity of DJ-1 has become a center of debate, making further studies necessary to better understand the possible link between DJ-1 and AGE formation, as well as the interplay between DJ-1 and metabolism. Here, we aimed to further explore the effects of DJ-1 loss in the murine metabolism across multiple tissues and under different diet interventions, as well as the potential DJ-1 deglycase activity both in mice and PD patient's fibroblasts. In brief, our results from DJ-1 knockout (KO) mice revealed a skeletal muscle atrophy resulting from a selective atrophy of the fast glycolytic type 2B fibers, and a resistance to diet-induced obesity under high-fat high-sucrose (HFHS) diet when compared to wildtype (WT). In addition, our metabolomics analysis identified the formation of three new glycerinyl-AGEs: α-glycerinylarginine (α-GR), α-glycerinyllysine (α-GK), and glycerinyltrimethyllysine (GTMK), specifically in the skeletal muscle from DJ-1 KO mice as well as in the fibroblasts of Park7-related PD patients. Thus, our study sheds light on a protective role of DJ-1 protein against AGE accumulation and skeletal muscle atrophy, while also identifying two new AGEs, α-GR and α-GK, as potential biomarkers for Park7-related PD patients.

INTRODUCTION

The multifaceted DJ-1 protein

DJ-1 protein and its regulation

First identified as an oncogene, the DJ-1 protein (Nagakubo et al., 1997) has increasingly become a focus of interest since it was first associated with early-onset Parkinson's disease (PD) in 2003 (Bonifati, 2003). DJ-1 is encoded by the PARK7 gene and it is nowadays known as a multifaceted antioxidative small protein present in most organisms from bacteria to human (Bandyopadhyay & Cookson, 2004; Bonifati, 2003; Lucas & Marín, 2007). Besides its association with cancer and early-onset familial parkinsonism, several studies have also shown that DJ-1 is involved in many other pathologies, such as stroke (Aleyasin et al., 2007; Yanagisawa et al., 2008) and type 2 diabetes mellitus (T2DM) (Jain et al., 2012), as well as neurodegenerative diseases such as sporadic PD (Bandopadhyay et al., 2004), Alzheimer's disease (AD) (Choi et al., 2006), Huntington's disease (HD) (Sajjad et al., 2014), and amyotrophic lateral sclerosis (ALS) (Lev et al., 2015). The exact mechanisms underlying these associations are not completely understood yet, but most of them, if not all, seem to have oxidative stress as a common denominator. However, to which extent the oxidative stress is directly involved in the association between DJ-1 and these diseases is also not clear as DJ-1 presents several other described functions.

Nevertheless, the activity and modulation of DJ-1 protein have been reported to occur through oxidation and post translation modification (PTM) of its cysteine residues, which are essential for DJ-1 functions and localization. Alongside a total of 189 amino acids, DJ-1 is also composed of three cysteine residues that are localized at the amino acid numbers 46 (C46), 53 (C53), and 106 (C106), with each of them presenting a different susceptibility to oxidation (Ariga et al., 2013). Among them, the C106 residue was reported as the most sensitive against oxidative stress and easily oxidised to SOH, SO_2H, and SO_3H, with SO_2H and SO_3H being considered as the active and inactive forms of DJ-1, respectively (Canet-Avilés et al., 2004; Kinumi et al., 2004; Taira et al., 2004).

Antioxidant function

The cellular redox homeostasis is an important and dynamic regulatory process that ensures a balance between reducing and oxidizing reactions to controls cell survival and biological responses in an oxygen environmental system. By activating a coordinated antioxidant cellular response, this system balances the formation of reactive oxygen species (ROS), which are primarily by-products of aerobic metabolism in the mitochondria. However, the presence of supraphysiological levels of ROS in the cells can lead to oxidative stress and damage in DNA and proteins, resulting in harmful cellular consequences and several diseases.

In this context, DJ-1 plays a major role against oxidative stress by acting both in a direct and indirect manner. As an example, by regulating specific transcription factors, DJ-1 can indirectly regulate the two most important antioxidant systems, the thioredoxin (Trx) and the glutathione (GSH) systems, to promote an optimal response to oxidative stress stimulus (Fu et al., 2009; Im et al., 2012; Raninga et al., 2014; W. Zhou & Freed, 2005). Moreover, DJ-1 also acts as antioxidant by regulating the activity of other transcription factors such as p53 (Fan et al., 2008) and NF-κB (McNally et al., 2011), which in turn regulate the expression of multiple genes involved in the response to oxidative stress; by activating superoxide dismutase 1 (SOD1), (Girotto et al., 2014; Wang et al., 2011), another important protein responsible for reducing free superoxide radicals in the cells; and by being involved in mitochondrial integrity (Knippenberg et al., 2013), which is essential for the mitochondria to play a crucial role in the cell maintenance and survival.

All the numerous described functional properties for DJ-1, including chaperone (Shendelman et al., 2004; W. Zhou et al., 2006), protease (J. Chen et al., 2010), and transcriptional regulator (Clements et al., 2006; Fan et al., 2008; McNally et al., 2011) contribute to its multifunctional role in the oxidative stress response. Indeed, it is believed that the antioxidant function of DJ-1 relies mostly on the binding and regulation of other proteins that are involved in cell survival, as for example the apoptosis signal-regulating kinase 1 (ASK1) and the p38-regulated/activated protein kinase (PRAK) (Waak et al., 2009; Im et al., 2010; Tang et al. 2014a). However, although oxidative stress is a common denominator among chronic diseases, it is still not clear to which extent this could be the underlying mechanism associated with the link between DJ-1 and diseases.

Neurodegenerative diseases

The association of DJ-1 with neurodegenerative diseases, more specifically with the autosomal recessive early-onset Parkinson's disease (Bonifati, 2003), has brought substantial attention to this protein and increased the number of studies involving DJ-1 over the past years. As a result, it is now known that this highly conserved and ubiquitously expressed DJ-1 protein plays an essential role as an antioxidative protein. Besides early-onset familial parkinsonism, DJ-1 was also associated with multiple system atrophy (MSA) and dementia with Lewy bodies (DLB), which are part of a group of diverse neurodegenerative disorders characterized by abnormal α-synuclein aggregation known as α-synucleinopathies. In these diseases, DJ-1 was reported to have a higher immunoreactivity in the brainstem of DLB and MSA patients, as well as in the cortex and cerebellum of the latter (Neumann et al., 2004; Rizzu et al., 2004). Although the underlying mechanisms are not completely elucidated yet, previous studies showed that DJ-1 can prevent the aggregation of α-synuclein through its chaperone activity (Shendelman et al., 2004; W. Zhou et al., 2006; Zondler et al., 2014) and regulation of heat shock protein 70 (W. Zhou & Freed, 2005), suggesting that this higher DJ-1 immunoreactivity could also be part of a regulatory defense mechanism.

DJ-1 was also associated with tau pathologies such as AD, in which hyperphosphorylated tau inclusions are known as major hallmarks (Neumann et al., 2004; Rizzu et al., 2004), and neuromuscular diseases such as ALS. In AD, DJ-1 was reported to be associated with neuronal and glial inclusions, which was suggested to indicate either a defense mechanism possibly linked with its antioxidant role, or a consequence of the disease resulting in DJ-1 being confined in the inclusions and not able to exert its functions (Kumaran et al., 2007; Neumann et al., 2004; Rizzu et al., 2004). In ALS patients, on the other hand, DJ-1 immunostaining signals presented a tissue-related difference, with motor cortex and skeletal muscle sections having stronger and lower signals, respectively, than their correspondent health controls (Knippenberg et al., 2013).

The association of DJ-1 with several neurodegenerative diseases, which impact a considerable part of the population, could be expect as DJ-1 is a conserved and ubiquitous protein that exerts a variety of crucial functions for cell maintenance and survival, as well as cell homeostasis. Thus, further understanding of DJ-1 functions, especially in a tissue specific manner, can contribute to elucidate the pathophysiology

of these diseases and in the search for biomarkers and new targets for drug development.

Parkinson's disease

Epidemiology

Considered the second most common age-related neurodegenerative disorder, PD affects approximately 3% of the population aged 65 or over, with its incidence and prevalence significantly increasing with aging (Pringsheim et al., 2014). Although mortality is not increased in the first decade after disease onset, it eventually doubles compared with the general population (Pinter et al., 2015). Nevertheless, the idea that PD exclusively affects elderly people is a misconception, and studies have shown that the onset of the disease can happen before 65 years old for almost 25% of the patients, and before 50 years old for 5-10% of them (Savica et al., 2013; Twelves et al., 2003; Van Den Eeden et al., 2003).

Although still not completely understood, both the incidence (number of new cases of the disease) and prevalence (number of existing cases) have increased rapidly in the past years, being considered as possibly the fastest growing neurological condition worldwide (Dorsey et al., 2018; GBD 2016 Neurology Collaborators, 2019). Importantly, incidence and prevalence seem to vary within subgroups defined by sex, race, ethnicity, genotype, and environment. For example, PD is generally twice as common in men than in women in most populations (Baldereschi et al., 2000; Van Den Eeden et al., 2003), leading to several theories that might explain this male prevalence, such as a protective effect of female sex hormones, a sex-associated genetic mechanism, sex-specific differences in exposure to environmental risk factors, as well as possible disparities in health care (Poewe et al., 2017). However, the complexity of both PD and these factors make it difficult to dictate the relative contribution to the risk of developing PD, resulting in controversial studies or insufficient data to exclude the effect of one or another.

Likewise, environmental factors are also known to modify the risks of developing PD, with its incidence significantly increasing in individuals exposed to traumatic brain injury (Camacho-Soto et al., 2017; Mackay et al., 2019) or to certain environmental

pollution with toxins, such as pesticides (e.g., paraquat) or chemicals (e.g., trichloroethylene), which are known to be harmful to PD-related neurons and brain circuits (Bloem et al., 2021). Curiously, the risk of developing sporadic PD seems to be lower in smokers or caffeine users (Ascherio & Schwarzschild, 2016). However, as previously mentioned, these associations are sometimes hard to interpret due to conflicting results, as well as a scarce number of studies. In this context, the negative association between PD risk and smoking, for example, could be false as smokers may have higher dopamine levels, which could prevent them to drop below a critically low dopamine threshold that is needed to manifest parkinsonism (Noyce et al., 2012; Rossi et al., 2018). Thus, further investigation of the interplay between environmental factors and lifestyle with risk of developing PD can contribute to better understanding the underlying mechanisms associated with this disease and consequently a better design of interventional studies aiming to delay or modify the course of PD.

Clinical diagnosis

Parkinson disease's diagnosis is clinically based and, except in selective cases in which genetic testing is performed, a definitive diagnosis is only stablished based on post-mortem identification of hallmark neuropathological changes in the brain (Bloem et al., 2021). The current criteria define PD as the presence of bradykinesia (i.e. slowness of movement and speed) together with at least rigidity or rest tremor (Kalia & Lang, 2015; Postuma et al., 2015; Tolosa et al., 2006) (**Figure 1**), which are part of what is known as cardinal motor features (Poewe et al., 2017). Besides these features, most PD patients also develop non-motor symptoms as for example sleep and mood disorders, cognitive impairment, and pain (Chaudhuri & Schapira, 2009), with some of these preceding the onset of classic motor symptoms and PD pathological hallmarks by years and being generally considered the start point for the decreased quality of life in these patients by adding considerably to overall burden. However, the manifestation of these symptoms and the patterns of disease progression are highly variable among patients, and even same symptoms such as resting tremor can have different impact among patient's quality of life depending on their occupation, for example. This heterogeneity in causes, manifestation, and personal priorities points to the need of more individual and targeted treatment approaches.

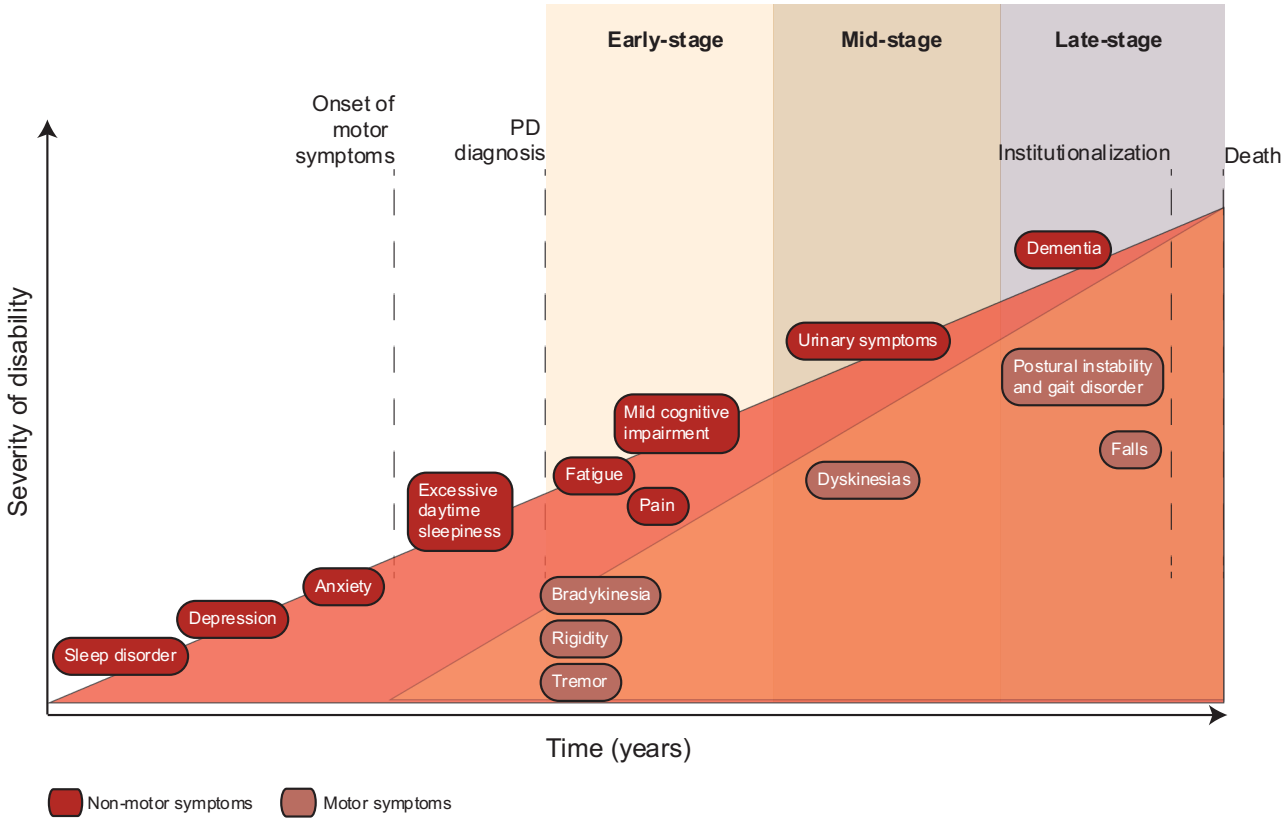

Figure 1. Clinical symptoms of Parkinson's disease. PD diagnosis occurs with the onset of motor symptoms. Non-motor symptoms are present throughout all stages of the disease at varying degrees and become increasingly prevalent over the disease progression. Adapted from Poewe et al., 2017.

Although the development of classical motor features suggests that clinical diagnosis may be straightforward, it is known that the earliest stages of PD can be difficult to recognise, reflected by the long average delay of 10 years that typically separates the person's first noticeable symptom from the timing of diagnosis (Gaenslen et al., 2011). Importantly, these delays are particularly common when tremor is absent, which may happen in up to 20% of patients with PD, and in early-onset PD patients (Ruiz-Lopez et al., 2019), highlighting the need for diagnostic tests and biomarkers to enhance diagnostic confidence in early disease.

Pathophysiology and risk genes

The first neuropathology hallmark ever described for PD over a century ago was the formation of Lewy bodies, which are mostly formed due to abnormal deposition and aggregation of α-synuclein in the cytoplasm of certain neurons in several brain regions (Braak et al., 2003). Moreover, PD is also mainly characterized by the loss of dopaminergic neurons in the substantia nigra pars compacta (SNpc), which causes striatal dopamine deficiency (Dijkstra et al., 2014). This loss of dopaminergic neurons is initially restricted to the ventrolateral substantia nigra with relative sparing of other midbrain dopaminergic neurons (Damier et al., 1999; Fearnley & Lees, 1991) in the early stage of the disease, becoming widespread by the end-stage of the disease. Although the causes are not yet completely understood, the pathophysiology of Parkinson's disease has shown to also be associated with a complex interplay among mitochondria dysfunction, lysosomes and vesicle transport, synaptic transport issues, and neuroinflammation (Kalia & Lang, 2015).

The projection of the dopaminergic neurons from the SNpc to the dorsal striatum, also known as the nigro-striatal pathway, plays a central role in the control of motor function. These neurons are responsible for the synthesis of the neurotransmitter dopamine, which occurs through the transformation of tyrosine to L-DOPA via the addition of a hydroxyl group, and subsequent removal of a carboxylic acid group from the ethyl side chain linked to the amine group (Z. D. Zhou et al., 2023). After its synthesis, dopamine is internalized into synaptic vesicles and stored until an action potential prompts the release of dopamine in the synaptic cleft, resulting in neuron communication through its binding to dopamine receptors on the postsynaptic neuron (Z. D. Zhou et al., 2023). However, the degeneration of dopaminergic neurons in this nigro-striatal pathway results in a decrease of dopamine synthesis and transmission, and the consequent dysregulation of motor control, a hallmark of PD (Bloem et al., 2021; Z. D. Zhou et al., 2023).

The extensive investigation in the field of PD's pathology and the advancement in the understanding of the contribution of dopaminergic neuron loss to the disease led to the development of efficient treatments for managing the disease symptoms. Moreover, the identification of genes associated with monogenic forms of PD, which represent around 5-10% of PD cases, also provided crucial clues to mechanisms underlying the neuropathology of PD. Genes such as Parkin RBR E3 ubiquitin-protein

ligase (PRKN), PTEN-induced putative kinase 1 (PINK1), Leucine-rich repeat kinas 2 (LRRK2), Parkinsonism associated deglycase (PARK7), ubiquitin carboxy-terminal hydrolase L1 (UCH-L1), β-glucocerebrosidase (GBA1), and synuclein alpha (SNCA), are known to be involved in a set of molecular pathways including α-synuclein (α-syn) proteostasis, mitochondrial function, oxidative stress, calcium homeostasis, axonal transport and neuroinflammation, and to have different frequency and penetrance in the PD pathology (Blauwendraat et al., 2020; Kalia & Lang, 2015).

The PARK7 gene, for example, is known to account for approximately 1% of PD cases (Taipa et al., 2016), while having a higher penetrance. Although the causal mechanisms between PARK7/DJ-1 and PD are not yet fully understood, PD patients are known to have increased oxidative stress in their brain (Dias et al., 2013). Indeed, according with the literature, the nigral dopaminergic neurons have been suggested to be particularly vulnerable to metabolic and oxidative stress due to several factors, as for example their particularly long unmyelinated axons with large numbers of synapses, which require great energy to be sustained (Bolam & Pissadaki, 2012; Pissadaki & Bolam, 2013), and their increased levels of cytosolic dopamine and its metabolites that can cause toxic oxidative stress (Lotharius & Brundin, 2002; Mosharov et al., 2009). However, it is not clear if this oxidative stress occurs earlier or later than the neuron degeneration, and further investigation of DJ-1 functions and associations with PD could contribute to the understanding.

Over the past years, significant strides have been made in the understanding of the neuropathology and progression of PD, as well as some important mechanisms and perturbations underlying the disease and its symptoms. Overall, some of the approaches for intervention in PD generally focus in targeting specific organelles, such as mitochondria or lysosomes, and associated proteins, as for example GBA1 and LRRK2, with unique downstream molecular influences that can be applied to specific subgroups of PD patients (Vijiaratnam et al., 2021). Alongside that, there are also some broader approaches that focus on targeting neuronal abnormalities that were shown to be commonly altered in PD patients such as α-syn production, cell-to-cell transmission, calcium signaling, and neuroinflammation (Vijiaratnam et al., 2021).

Although highly efficacious therapies such as levodopa (L-DOPA) treatment and deep brain stimulation (DBS) have become available, understanding how to delay disability and modify disease progression is still critical, since none of these treatments

are curative and PD remains a progressive disorder that eventually causes severe disability. Likewise, there is also a need for finding specific and sensitive biomarkers that can be used to assess disease risk and progression, as well as contribute to early diagnosis. In this context, previous studies have attempted to define diagnostic markers for the earliest stages of the disease by trying to detect α-synuclein-related pathology in skin punch biopsies (Mahlknecht et al., 2015). Moreover, the advance of omics techniques has allowed the identification of small changes in protein, metabolite, or RNA profiles in fluids and tissue from patients and healthy individuals (Delenclos et al., 2016), making them a powerful tool in the search for biomarkers.

Metabolism

Among all its functions, DJ-1 was also shown to be involved in metabolism, a set of basic and fundamental chemical reactions that occur physiologically to produce energy from food. Although the complete mechanism is not yet elucidated, DJ-1 has been proposed to be involved in the metabolism of different tissues, as for example pancreatic islets (Jain et al., 2015), adipose tissue (Kim et al., 2014; Shi et al., 2015), and skeletal muscle (Shi et al., 2015), which are all highly active metabolic organs. However, investigating the effects of DJ-1 loss in the metabolism requires a systematic analysis across different metabolically active tissues to better understand the underlying mechanisms associated to the interplay of DJ-1 and metabolism. Currently, most available studies focus on specific tissues, making it hard to understand the extent of the DJ-1 function in the overall metabolism or its tissue-specific function.

Diabetes and obesity

Characterized by insulin resistance and dysfunction of insulin-producing beta cells (Samuel et al., 2010; Shulman, 2014; Sun et al., 2011), type 2 diabetes mellitus (T2DM) is considered the most common type of diabetes. This inadequate insulin production due to islet dysfunction or beta cell loss, alongside reduced glucose uptake in peripheral tissues, such as skeletal muscle, liver, and adipose tissue, result in what is known by impaired glucose tolerance. Alongside obesity and other conditions, this insulin resistance is part of what is also known as metabolic syndrome (MetS), a

common and growing public health problem that has been associated with increased risk of several chronic diseases worldwide, including stroke, heart diseases, diabetes, and some neurodegenerative ones.

Importantly, increased oxidative stress is a common pathophysiological process shared between MetS and diseases such as PD (Aviles-Olmos et al., 2013; Perry, 2004; Stark & Roden, 2007), reinforcing the need of further investigation of DJ-1 protein functions. Besides that, the link between DJ-1 and metabolism, as well as the identification of other PD associated genes that are responsible for encoding proteins that regulate lipid metabolism, as for example GBA1, show that lipids and metabolism may play an important role in the pathophysiology of PD (Clark et al., 2007; Nichols et al., 2009). As previously reviewed (Fanning et al., 2020), more recent studies have suggested that PD may not be only a proteinopathy but also lipidopathy, increasing the relevance of further understanding the interplay between metabolism and neurodegenerative diseases.

Regarding the effects of DJ-1 loss in the metabolism, a previous study showed that DJ-1 KO mice were more insulin sensitive and glucose tolerant compared to controls in response to a high-fat diet (HFD), as well as resistant to diet-induced obesity (Shi et al., 2015), suggesting an overall protective metabolic effect due to DJ-1 loss. However, further investigation of the effects of DJ-1 in other tissues such as skeletal muscle is still needed to better understand the potential protective or detrimental effects of DJ-1 loss. According with the literature, skeletal muscle accounts for most of the postprandial glucose uptake in humans and rodents (Merz & Thurmond, 2020), making it an extremely important tissue to further understand its role in metabolism under not just health but also pathological conditions such as T2DM and obesity, which are closely related (Samuel et al., 2010; Shulman, 2014; Sun et al., 2011). Importantly, DJ-1 was suggested to promote efficient fuel utilization through its role in ROS signaling (Seyfarth et al., 2015; Shi et al., 2015), which was previously reported to be beneficial at higher levels in the skeletal muscle since it was encountered in conditions associated with increased life span, as for example exercise (Tiganis, 2011). However, a more precise link of how DJ-1 modulates fuel utilization in the skeletal muscle remains to be addressed, especially when considering the importance of skeletal muscle for the overall systemic metabolism.

Glycation and the formation of advanced glycation end products (AGEs)

As a physiological consequence of metabolism, the spontaneous age-dependent posttranslational modification known as glycation can lead to the formation of Shiff bases, Amadori products, and advanced glycation end products (AGEs) (Rabbani et al., 2016; Richarme et al., 2015), with an ultimate impact in the structure and function of several proteins (Richarme et al., 2018). The formation of AGEs, a heterogeneous group of compounds, occurs physiologically in all tissues and body fluids (J.-H. Chen et al., 2018), and has received increased attention since its accumulation has been associated with chronic diseases such as diabetes mellitus, cardiovascular and neurodegenerative diseases, as well as with cancer, skeletal muscle atrophy and the aging process (Luevano-Contreras & Chapman-Novakofski, 2010). The most known mechanism of AGE formation, the Maillard reaction, occurs when reducing sugars such as glucose react in a non-enzymatic way with amino acids in proteins, with lipids, or with DNA (Luevano-Contreras & Chapman-Novakofski, 2010) (**Figure 2**).

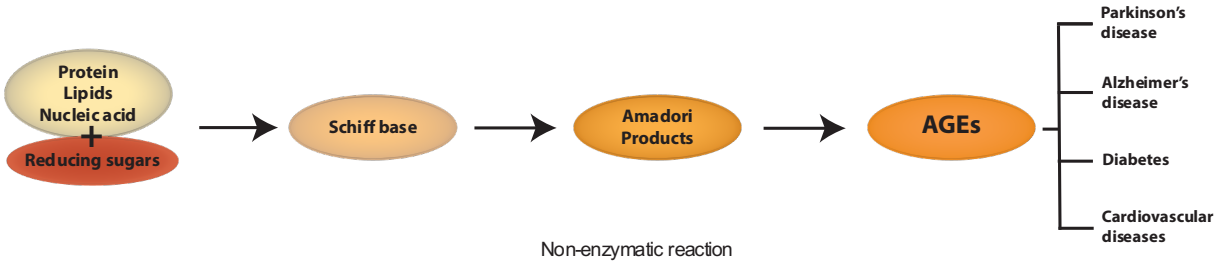

Figure 2. Advanced glycation end products (AGEs) formation. The formation of AGEs occurs mainly through the Maillard reaction. Created based on de Vos et al., 2016, licensed under the terms of the Crative Commons CC-BY.

In this classical pathway, the interaction between the carbonyl groups (C = O) of reducing sugars with amino groups of proteins results in the formation of Shiff bases. This reaction can happen within hours depending on the concentration of glucose and can also be reversible if the concentration of glucose decreases. Next, Schiff base goes into an intramolecular rearrangement that results in more stable compounds, known as Amadori products. One very important example of an Amadori product is the

glycated hemoglobin, which is widely used in clinics for long term control of blood glucose levels in diabetic patients (Monnier & Sell, 2006). Lastly, Amadori products go into a slow process of oxidation that results in reactive carbonyl compounds and subsequently the formation of AGEs, as for example pentosidine and Nε-carboxymethyl-lysine (CML) (Monnier & Sell, 2006).

The formation of AGEs can also occur through lipid peroxidation at both extra and intracellular levels, and through the glycolysis pathway, which leads to intracellular AGEs formation (**Figure 3**). During the intracellular glycolysis pathways, glucose is altered into reactive carbonyl compounds such as methylglyoxal, which can then react with proteins and result in AGEs formation (Lc et al., 2016).

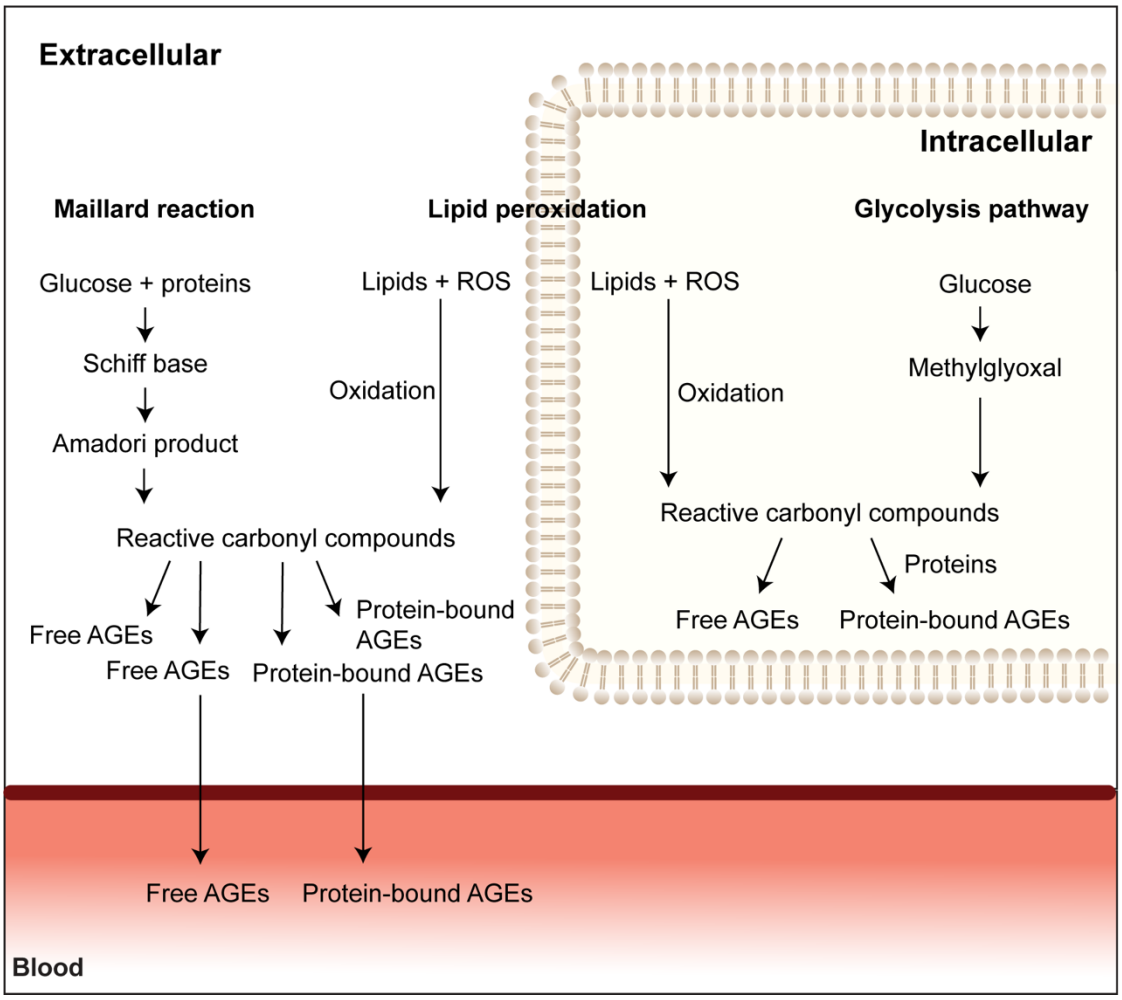

Figure 3. Pathways associated with AGEs formation. The AGEs formation can occur through the Maillard reaction, lipid peroxidation, or glycolysis pathway. Adapted from de Vos et al., 2016, licensed under the terms of the Crative Commons CC-BY.

Besides the previously described roles, DJ-1 was more recently proposed to also act as a deglycase (Richarme et al., 2015), avoiding the formation of AGEs. By acting on early glycation intermediates, DJ-1 seems to repair methylglyoxal (MGO) (CH_3-CO-CHO) and glyoxal (GO) (CHO-CHO)-glycated amino acids and proteins, releasing lactate and glycolate, respectively (Richarme et al., 2018). However, DJ-1 deglycase activity has recently become center of debate, with studies claiming that this apparent activity was rather due to TRIS buffer artifact (Pfaff et al., 2017a), since TRIS can affect the MGO/hemithioacetal equilibrium, or due to a shift in equilibrium caused by an actual DJ-1 glyoxalase activity, which removes the free MGO and results in

subsequent decomposition of hemithioacetal and aminocarbinols (Andreeva et al., 2019).

Nevertheless, the potential involvement of DJ-1 in AGE clearance requires further attention as AGEs have been linked with several diseases, including PD. According with a previous study, AGEs and α-synuclein are similarly distributed in very early Lewy bodies in human brain with incidental Lewy body diseases, i.e. control patients that show Lewy bodies in the substantia nigra (SN) (Münch et al., 2000). Since the autopsy was performed before the possible development of clinical signs of PD, these cases can be viewed as pre-Parkinson patients, suggesting that AGE-associated Lewy bodies formation seem to reflect early rather than late changes of PD (Münch et al., 2000). Moreover, AGEs have been suggested to be a major structural crosslinker that can transform soluble neurofilament proteins into insoluble aggregates (Richarme et al., 2018), indicating that the possible DJ-1 deglycase activity could represent one of the mechanisms linked to Park7-related PD cases. However, further studies are needed to explore to which extent they are associated.

As one can expect, the rate of AGEs formation in vivo can be influenced by several factors, as for example the nature and concentration of the substrate groups, the presence of glycating agents, the half-life of the proteins, and the oxidative stress or redox balance of the environment (J.-H. Chen et al., 2018). Although the complete mechanisms are not yet fully elucidated, the vast amount of data in the literature support the association of AGEs accumulation with organ function decline (Luevano-Contreras & Chapman-Novakofski, 2010). Thus, restoring redox homeostasis and AGE clearance have been considered possible therapeutic strategies against both metabolic and neurodegenerative diseases. However, without knowing both the molecular basis and mechanisms of DJ-1 function, which have been associated with both metabolic changes and PD, current therapeutic strategies for these disorders remain untargeted and therefore mostly ineffective.

AIMS

The first association between the PARK7 gene and early-onset familial parkinsonism in 2003 raised attention to the DJ-1 protein, increasing the number of studies and the knowledge about this protein. Since then, several studies have shown that DJ-1 plays an important role in oxidative stress and MetS, such as diabetes and obesity, which are associated with PD. However, the importance of DJ-1 in the interplay between metabolism and PD, two very complex systems, is still controversial and needs further investigation. Moreover, while DJ-1 deglycase activity has become a center of debate recently, AGEs are known to have detrimental effects in the physiological system and to be involved in several pathologies such as diabetes complications and neurodegenerative diseases. Thus, in this thesis, we aimed to:

1. Explore the systemic effects of DJ-1 loss in the murine metabolism.
2. Investigate the deglycase activity of DJ-1 in vivo.
3. Identify potential future biomarkers for Park7-related PD cases.
4. Validate the DJ-1 deglycase activity, and potential biomarkers, in Park7-related Parkinson's disease patients' samples.

MATERIAL AND METHODS

Animals, diet, and sample collection

DJ-1 KO mice were generated by gene trap insertion as previously described elsewhere (Pham et al., 2010). Male mice were housed at 23°C under a 12hr light-dark regimen with free access to water and food, either standard chow diet (#1310, Altromin, Germany) or high-fat high-sucrose diet (58% kcal from fat and sucrose, Research diets, D12331), for 12 weeks. Six months old mice were euthanized by cervical dislocation ~3-4 hours after the start of the light phase (~9am-10am). Tissues were immediately collected, snap frozen in liquid nitrogen, and stored at -80 °C until subsequent use.

Animal experiments complied with the European directive 2010/63/EU of the European Parliament and were approved by the local animal welfare authority in Germany (District government of upper Bavaria No.55.2-1-54-2532-94-2012. Wildtype and PARK7 knockout mice on a C57BL6/J background (Park7_XE726_GT) were bred and maintained at the animal facilities of Helmholtz Munich.

Indirect calorimetry and metabolic phenotyping

Total body fat and lean tissue mass were quantified by nuclear magnetic resonance (EchoMRI). Food intake, locomotor activity, energy expenditure, and respiratory exchange ratio (RER) were all monitored on a TSE system (Bad Homburg, Germany).

Immunofluorescence

Cryosections of gastrocnemius muscles were stained with rabbit polyclonal antibody against laminin (L9595, Sigma-Aldrich, 1:100 dilution) and monoclonal anti-myosin heavy chain (MyHC) antibodies produced in the laboratory of Stefano Schiaffino (Schiaffino et al., 1989), and distributed by the Developmental Studies Hybridoma Bank (DSHB, University of Iowa): BA-D5 (IgG2b, supernatant, 1:100 dilution) specific for MyHC-I, SC-71 (IgG1, supernatant, 1:100 dilution) specific for MyHC-2A, and BF-F3 (IgM, purified antibody, 1:100 dilution) specific for MyHC-2B. Type 2X fibers are not

recognized by these antibodies, and so appear black. Four different secondary antibodies (Jackson ImmunoResearch) were used to selectively bind to each primary antibody: goat anti-rabbit, conjugated with Alexa 647 fluorophore; goat anti-mouse IgG1, conjugated with DyLight488 fluorophore (to bind to SC-71); goat anti-mouse IgG2b, conjugated with DyLight405 fluorophore (to bind to BA-D5); goat anti-mouse IgM, conjugated with Alexa594 fluorophore (to bind to BF-F3). Muscle cryosections, 8µm thick, were incubated with M.O.M. IgG blocking solution (Vector Laboratories) for 1 hour at room temperature, then briefly rinsed once with phosphate-buffered saline (PBS). A solution with all the primary antibodies in PBS containing 1% of bovine serum albumin (BSA) was then prepared, and sections were incubated overnight at 4°C. After 3 washes of 5 minutes with PBS, sections were incubated for 30 minutes at 37°C with a solution with the four different secondary antibodies, diluted in PBS containing 1% of BSA and 5% of goat serum. After washing 3 times again with PBS for 5 minutes each and a brief rinse in water, sections were mounted with a saturated solution of ethyl-vinyl alcohol in PBS with 30% glycerol. A control incubation with no primary antibodies was performed, as well as control incubations with each primary antibody and non-specific secondary antibodies to exclude any possible cross-reaction. Pictures were collected with an epifluorescence and stage-motorized Leica DM6 B microscope, equipped with a Leica DFC 7000T camera. Single-color images were merged to obtain a whole muscle reconstruction with Leica LASX software, and images were analyzed with MATLAB using SMASH application (https://pubmed.ncbi.nlm.nih.gov/25937889/)

Reversed phase-ultrahigh-performance liquid chromatography (RP-UHPLC)-tandem mass spectrometry

Gastrocnemius muscle samples were randomized and homogenized with 1.4 mm ceramic beads in water (15 µL/mg) at 4 °C as previously described (Artati et al., 2022). For metabolite extraction and protein precipitation, 500 µL methanol extraction solvent containing recovery standard compounds was added to each 100 µL of tissue homogenate. Supernatants were aliquoted and dried under nitrogen stream (TurboVap 96, Zymark, Hopkington, MA, USA), and stored at -80°C until the UPLC-MS/MS measurements were performed. Two aliquots, one early and one late eluting compound, were dedicated for analysis by UPLC-MS/MS in electrospray positive

ionization and one for analysis by UPLC-MS/MS in negative ionization. Three types of quality control samples were included in each plate: samples generated from a pool of human ethylenediamine tetraacetic acid (EDTA) plasma, pooled sample generated from a small portion of each experimental sample served as technical replicate throughout the data set and extracted water samples served as process blanks. Prior to UPLC-MS/MS analysis, the dried samples were reconstituted in acidic or basic LC-MS-compatible solvents, each of which contained eight or more isotopically labeled standard compounds at fixed concentrations to ensure injection and chromatographic consistency. The UPLC-MS/MS platform utilized a Waters (Milford, MA, USA) Acquity UPLC with Waters UPLC BEH C18-2.1 mm × 100 mm, 1.7 µm columns, a Thermo Scientific (Waltham, MA, USA) Q Exactive high resolution/accurate mass spectrometer interfaced with a heated electrospray ionization (HESI-II) source, and N Orbitrap mass analyzer operated at 35,000 mass resolution. One aliquot of the extracts was reconstituted in acidic positive ion conditions, chromatographically optimized for more hydrophilic compounds (for early eluting compounds). In this method, the extracts were gradient eluted from the C18 column using water and methanol containing 0.05% perfluoropentanoic acid (PFPA) and 0.1% formic acid (FA). Another aliquot that was also analyzed using acidic positive ion conditions but was chromatographically optimized for more hydrophobic compounds (for later eluting compounds), was gradient eluted from the same C18 column using methanol, acetonitrile, and water; containing 0.05% PFPA and 0.01% FA and was operated at an overall higher organic content. The basic negative ion condition extracts were gradient eluted from a separate C18 column using water and methanol containing 6.5 mM ammonium bicarbonate at pH 8. The MS analysis alternated between MS and data dependent MS2 scans using dynamic exclusion and a scan range of 80–1000 m/z. Metabolites were identified by automated comparison of the ion features in the experimental samples to a reference library of chemical standard entries that included retention time, molecular weight (m/z), preferred adducts, and in-source fragments as well as associated MS spectra and curation by visual inspection for quality control using proprietary software developed by Metabolon Inc. Only fully annotated metabolites were included for further evaluation. Data were normalized according to raw area counts, and then each metabolite scaled by setting the median equal to 1. Features with >40% missing values were removed and remaining missing values (7%) were imputed with k-nearest neighbors algorithm. Biochemicals labelled with an asterisk (*) indicate compounds

that have not been officially confirmed with a standard, but we are confident in its identity.

Hydrophilic interaction liquid chromatography (HILIC)-tandem mass spectrometry

Mouse gastrocnemius muscle, brain, liver, and plasma samples were analyzed. A total of 200mg of 1mm zirconium beads was added to a 2.0mL impact resistant tube and placed on dry ice to pre-chill the tube. Tissue samples were then weighed, placed into the tube, and 1.0mL of cold 80:20 methanol (Honeywell-Burdick & Jackson LC230-4):water (Fisher Chemical W6-4) was added. Tissue samples were homogenized by three 15 second homogenization cycles at 6,400Hz in a Precellys 24 tissue homogenizer (Bertin Corp). Liver and brain samples underwent one homogenization cycle and muscle samples underwent two, with a one-minute cooling step on dry ice in between. After homogenization, samples were placed in the -20°C freezer for 30 minutes to allow for precipitation of protein. Samples were vortexed, transferred to a 1.5mL Eppendorf tube, and centrifuged at 14,000rpm at 4ºC for 10 minutes. The supernatant was taken to a clean tube and immediately dried in vacuo using a Thermo Savant vacuum concentrator operated at 35ºC. Once dry, samples were resuspended in a normalized volume of 80:20 methanol:water to result in a final concentration of 55μg/μL for muscle and liver samples and 61μg/μL for brain samples. Plasma samples were prepared by adding 160μL of cold methanol to 40μL of plasma. Samples were vortexed for 30 seconds and then placed in the -20°C freezer for 30 minutes. Thereafter, samples were centrifuged at 14,000rpm at 4ºC for 10 minutes and the supernatant was transferred and immediately dried in vacuo using a Thermo Savant vacuum concentrator operated at 35ºC. Plasma samples were resuspended in 80:20 methanol:water. Tissue and plasma samples were transferred to LC-MS vials containing a 200 μl glass inserts and were kept at 4ºC in the autosampler compartment until they were injected for analysis.

For tissue samples and plasma samples, 2μl and 1μl respectively, were injected on a Thermo QExactive orbitrap mass spectrometer coupled to a Thermo Vanquish UPLC system. Samples were randomized to alternate WT and KO conditions. To analyze polar molecules, chromatographic separation was achieved using a Millipore

(Sequant) Zic-pHILIC 2.1x150mm 5um column maintained at 25ºC with a flow rate of 0.3mL/min. A 19-minute linear gradient starting from 90:10 acetonitrile (Honeywell-Burdick & Jackson LC015-4):20mM ammonium bicarbonate (Fluka 1066-33-7) to 45:55 acetonitrile:20mM ammonium bicarbonate was used to elute compounds. The Thermo Q-Exactive orbitrap mass spectrometer was operated in positive and negative ion modes using a heated electrospray ionization (HESI) source at 35,000 resolution,100ms ion trap time for MS1 and 17,500 resolution, 50ms ion trap time for MS2 collection. We collected data over a mass range of m/z 67-1000. We used an auxiliary gas flow rate of 20 units, sheath gas flow rate of 40 units, sweep gas flow rate of 2 units, spray voltage of 3.5 and 2.5 kV for positive and negative ion modes (respectively), capillary inlet temperature of 275ºC, auxiliary gas heater temperature of 350ºC and an S-lens RF level of 45. All MS1 ions were isolated using a 1.0 m/z window for MS2 collection and fragmented using a normalized collision energy of 35. These fragmented ions were placed on dynamic exclusion for 30 seconds before being allowed to be fragmented again. For analysis, we imported collected data into the mzMine 2.20 software suite. Pure standards were used for identification of metabolites through manual inspection of spectral peaks and matching of retention time and MS1 accurate mass, with confirmation of identification through comparison to MS/MS fragmentation patterns.

Amide-AGE determination and validation by LC-MS/MS

Materials

L-arginine (≥98%) and L-lysine (≥98%) were purchased from Sigma-Aldrich (Steinheim, Germany). N-ε-glycerinyllysine was purchased from Iris Biotech GmbH (Marktredwitz, Germany). Milli-Q purified water was from a Milli-Q Integral Water Purification System (18.2 MΩ, Millipore, Germany). Acetonitrile, methanol, and 2-propanol (all hypergrade for LC-MS) were purchased from Merck (Darmstadt, Germany). Formic acid (98%, for mass spectrometry) was obtained from Honeywell Fluka (North Carolina, USA). Ammonium formate solution 10 M in water (BioUltra grade) was supplied by Sigma Aldrich (Steinheim, Germany). The API-TOF Reference Mass Solution Kit and ESI-L Low Concentration Tuning Mix were purchased from Agilent Technologies (Waldbronn, Germany).

Model system preparation

For preparation of reference $^{13}C_3H_4O_3$-modified amino acids, model systems were prepared from amino acids, namely arginine and lysine, and D-glucose-$^{13}C_6$. Aqueous stock solutions (0.2 M) of glucose and each amino acid were mixed 1:1 (*v*/*v*), respectively. Glucose and amino acid standard solutions in Milli-Q purified water (0.1 M) were prepared as control samples. Samples were heated in closed glass vials for 2 h at 100 °C according to the protocol recently described (Berger et al., 2022). Glycation products without isotopic tags were prepared analogously using regular D-(+)-glucose.

Sample preparation

Skeletal muscle samples were weighed in pre-cooled NucleoSpin Bead Tubes (Macherey-Nagel, Düren, Germany) and homogenized in ice-cold 70:30 methanol:water (15 µL/mg tissue) by the addition of grinding beads at 7,200 rpm for 4 min using a Precellys Evolution Homogenizer (Bertin Corp., Rockville, Maryland, USA). Homogenates were transferred and empty extraction tubes and washed with 100 µL 70:30 methanol:water. Protein was precipitated from the homogenates by addition of pure methanol (75:25 methanol:water). Homogenates were cleared by centrifugation at 13,000 rpm at 4 °C for 15 min. The supernatant was evaporated to dryness and resuspended in 80:20 acetonitrile:water (2 µL/mg tissue). After centrifugation at 13,000 rpm and 4 °C for 15 min, the supernatant was transferred to LC-MS vials for mass spectrometric analysis.

Fibroblast samples were handled on dry ice during all procedures. For homogenization, 960 mg of glass beads (diameter 0.5 mm, PeqLab) and 2 g of ceramic beads (diameter 1.4 mm, Peqlab) were added to each sample. Cell suspensions were homogenized at 5,500 rpm for 13.3 min using a Precellys Evolution Homogenizer (Bertin Corp., Rockville, Maryland, USA). Homogenates were cleared by centrifugation at 20,000 × g and 4 °C for 15 min. The supernatant was evaporated to dryness and resuspended in 70 µL Milli-Q purified water. To ensure conditions were above limit of detection four replicates per individual were pooled. After centrifugation at 20,000 × g and 4 °C for 10 min, the supernatant was transferred to LC-MS vials for

mass spectrometric analysis. To normalize metabolomics data to cell number, fluorometric determination of DNA levels was performed using small aliquots of the homogenates as descried before (Muschet et al., 2016). The remaining homogenates were used for the extraction of metabolites.

LC-MS/MS analysis

Prior to measurement, model systems were diluted 1:10 (v/v) with 80:20 acetonitrile:water. Fibroblast and muscle extracts were measured undiluted. Samples were randomized, and analyzed by a UHPLC (1290 Infinity II, Agilent, Waldbronn, Germany) coupled to a drift tube ion mobility (DTIMS) quadrupole time-of-flight (QToF) mass spectrometer (6560B, Agilent, Waldbronn, Germany). For hydrophilic interaction liquid chromatography (HILIC), a ZIC-cHILIC column (100 x 2.1 mm, 3 µm, 100Å, zwitterionic, Merck, Darmstadt, Germany) was used. Samples were injected via partial-loop injection (10 µL). The flow rate was set to 0.5 mL/min and the column temperature was maintained at 40 °C. HILIC separation was run in gradient mode. Initial conditions were set to 0.01% eluent A (acetonitrile:water, 5:95 (v/v), 5 mM ammonium formate, 0.1% formic acid) and 99.9% eluent B (acetonitrile:water, 95:5 (v/v), 5 mM ammonium formate, 0.1% formic acid). After 2 min, eluent B was decreased to 56% over the next 11 minutes. Eluent B reached 30% within 1 min and finally 10% after additional 0.1 min. This composition was maintained to the end of the run. The gradient was completed after 18.1 min. The MS was operated in positive electrospray ionization (ESI) mode within a mass range of 50-1700 m/z using QToF-only mode. External calibration and system tuning was performed using an ESI-L Low Concentration Tuning Mix solution prior to analysis and each MS spectrum was automatically recalibrated by continuously delivered API-TOF Reference Mass solution (purine m/z 121.0509 and HP-921 at m/z 922.0098) during analysis. The settings of the ion source were: capillary voltage 4000 V, nozzle voltage to 10 V, dry gas temperature 250 °C, dry gas flow 12 L/min, nebulizer pressure 40 psi, sheath gas temperature 250 °C, sheath gas flow rate 11 L/min (both gasses nitrogen). Mass spectra were acquired with a scan rate of 8 Hz in data-dependent mode and the three highest MS^1 ions per precursor scan were fragmented using a normalized collision energy of 20 eV. Raw data were post-processed using GeneData Expressionist Refiner MS 13.5 (GeneData GmbH, Basel, Switzerland) applying chemical noise subtraction, intensity cutoff filter,

chromatographic peak picking, isotope clustering, and retention time alignment. Further processing was performed in R software (version 4.1.3).

Consensus Spectra Computation

Consensus MS/MS spectra were computed with the R package MSnBase using the consensusSpectrum() function (Gatto & Lilley, 2012). We retained mass peaks present in a minimal proportion of 5% of spectra in the final consensus spectra. For peak aggregation, a maximum m/z merge distance of 0.005 Da was applied, and intensities of merged peaks were summed.

Sequence alignments of human fibroblasts

Genomic DNA was isolated from fibroblasts using the DNeasy Blood & Tissue Kit (Qiagen) according to the manufacturer's instructions. To verify the PARK7 insertion mutation of Patient 1, exon 1 of PARK7 was PCR amplified using the intron/exon overlapping primers hPARK7_Ex1_for: 5'–TTTTTAAGGCTTGTAAACATATAAC-3' and hPARK7_Ex1_rev: 5'–GACTTACCCCAGCTCGC-3'. Polymerase chain reaction (PCR) products of around 130 bp were cloned into the pCRII-TOPO vector according to the manufacturer's instructions. Inserted sequences were verified by Sanger sequencing using standard M13 forward and reverse vector primers. To verify the PARK7 deletion mutation of Patient 2, exon 7 of PARK7 was PCR amplified from genomic DNA using the intronic primers hPARK7_Ex7_for1: 5'-CTGAAGGAGCAAGGAACTGGA-3' and hPARK7_Ex7_rev1: 5'-GGAATGCTGGGTGCTATTACCT-3' as previously described (Mencke et al., 2022). The resulting PCR products of around 1860 bp were purified by PCR Purification Kit (Macherey Nagel) and Sanger sequenced using the nested primers hPARK7_Ex7_for2: 5'-GCCCATTAGGATGTCACCTTT-3' and hPARK7_Ex7_rev2: 5'-GCAGTTCGCTGCTCTAGTCTT-3' as previously described (Mencke et al., 2022). Sequences were analyzed by the software SnapGene and sequence alignment performed using Clustal Omega (https://www.ebi.ac.uk/Tools/msa/clustalo/).

Western blot of PARK7 in human cells

HEK293 cells overexpressing recombinant PARK7 from a pLX304-hPARK7 E176G plasmid were generated as previously described (Tokarz et al., 2020). Aliquots of 1 x 10^6 fibroblasts were suspended in 100 µL lysis buffer (20 mM Tris-HCL, 150 mM NaCl, 1 mM EDTA, 1 mM EGTA, 1% Triton X-100, pH 7.5) supplemented with phosphatase inhibitor PhosSTOP and protease inhibitor C0mplete (Roche) and lysed by sonication in a sonication bath (3 cycles with 10 sec in sonication bath and 20 sec on ice). Total protein content was determined by Bradford assay (Bio-Rad) using BSA as reference protein (Bradford, 1976). 20 µg of fibroblast lysate or 5 µg of HEK293 lysate were subjected to SDS-PAGE on a precast 4-15% TGX Tris-Glycine Stain-Free Gel (Bio-Rad). Separated proteins were transferred within 30 min at constant voltage of 20 V to an Immobilon FL PVDF membrane (Millipore) using the Semi-Dry Transblot instrument (Bio-Rad). After blocking the membrane in 5% milk powder in Tris-Buffered Saline (TBS), the membrane was simultaneously incubated for 2 h at room temperature (RT) with the primary monoclonal antibodies rabbit-anti-DJ-1 (D29E5) XP® (Cell Signaling #5933) and mouse-anti-beta-tubulin TUB2.1 (Sigma #T5201), both at a dilution of 1:1000 in 2.5% milk powder in TBS-T (0.1% Tween-20). After thorough washing with TBS-T (0.1% Tween-20), the blot was incubated overnight at 4°C with the secondary antibodies goat anti rabbit-HRP (Sigma #A6154) and goat anti mouse-HRP (Dianova #115-035-068) at a dilution of 1:20000 each in 2.5% milk powder in TBS-T (0.1% Tween-20). After several washing steps, enhanced chemiluminescence (ECL) signals were generated using the Pierce ECL 2 Western Blotting Substrate (Pierce) according to the manufacturer's instructions and detected using a Fusion FX6 Edge (Vilber Lourmat).

Fibroblast cell culture

Fibroblasts derived from human skin from patients and controls kindly donated by Prof. Dr. Vicenzo Bonifati (Department of Clinical Genetics, Erasmus MC, University Medical Center Rotterdam, Rotterdam, The Netherlands) were maintained in high glucose (4.5 g/L glucose, Gibco) DMEM (Dulbecco's Modified Eagle Medium) supplemented with 10% fetal bovine serum (FBS Superior, Biochrom) and 100 units/mL of penicillin and 100 µg/mL streptomycin (Gibco) at 37 °C and 5% CO_2 in a

humidified atmosphere. Cells were frequently monitored to be free of mycoplasma contamination using the MycoAlert™ mycoplasma detection kit (Lonza) and the MycoAlert™ assay control set (Lonza).

For expression and mutation verification analyses, cells were harvested by trypsinization, washed once in warm PBS, and counted by using the Cellometer Auto T4 Plus (PeqLab). Cells were pelleted into aliquots containing 1 x 10^6 cells and stored at -80 °C until further use.

For amide-AGE determination by LC-MS/MS, 7 x 10^5 cells were seeded into culture dishes (diameter 10 cm) with either 12 mL of DMEM high glucose (4.5 g/L glucose, Gibco) or 12 mL of DMEM low glucose (1 g/L glucose, Gibco) supplemented with FBS and penicillin/streptomycin as described above. Cells were grown for 3-5 days to reach confluence of ~80%. For harvesting, cells were washed twice with 13 mL of warm PBS before their metabolism was quenched by adding 3 mL of ice-cold extraction solvent (80/20 (v/v) methanol/water). Cells were then scraped off the culture dishes using rubber tipped cell scrapers (Sarstedt) and together with extraction solvent collected in 7 mL PeqLab tubes (cells and solvent of two 10 cm dishes were pooled in one tube) and stored at -80 °C until further use.

Statistical analyses

Sample sizes for mouse experiments were 5-7 per genotype. Data were analyzed by two-tailed unpaired Student's t-test or two-way ANOVA, followed by Bonferroni's multiple comparisons test, as appropriate, using GraphPad Prism version 9. To statistically assess differences in metabolite intensities among experimental conditions, t-tests (unpaired, two-sided) were performed using the t.test() function from the stats R package. Data was subjected to log transformation and missing value imputation, if any, with a random number between minimum values across samples. The p values were corrected for multiple testing using the Benjamini-Hochberg method as implemented in the R function p.adjust(). Differences between two groups were considered statistically significant for $p < 0.05$.

MetaboAnalyst

Enrichment analysis of altered metabolites was performed using MetaboAnalyst 4.0 (Chong et al., 2019) with default parameters and Kyoto Encyclopedia of Genes and Genomes (KEGG) IDs. Quantitative Enrichment Analysis was performed via the Enrichment Analysis module using the pathway based KEGG metabolite set library (84 metabolite sets based on human metabolic pathways).

RESULTS

Experiments performed in DJ-1 animal model

DJ-1 loss results in resistance to diet-induced obesity, decreased fat free mass and muscle atrophy in male mice

To investigate the effects of DJ-1 loss in whole body metabolism under a chronic metabolic stress, we used littermates DJ-1 knockout (KO) and wild type (WT) mice fed with a high-fat high-sucrose (HFHS) diet for 12 weeks. At the end of this period, WT mice exhibited a significantly higher bodyweight (BW) compared to DJ-1 KO mice fed with the same diet **(Figure 4A)**. This difference in BW was accompanied by the expected gain of total fat mass **(Figure 4B)** and higher epididymal white adipose tissue (eWAT) mass **(Figure 4C)** only in WT mice, indicating that DJ-1 KO mice were resistant to diet-induced obesity (DIO). Moreover, echoMRI analysis also showed that DJ-1 KO mice presented reduced fat free mass **(Figure 4D)**, suggesting potential differences in muscle mass. To start exploring the effects of DJ-1 loss in the skeletal muscle, we measured the mass of gastrocnemius muscle from WT and DJ-1 KO mice under HFHS diet. Indeed, we found a significant decrease in the mass of gastrocnemius muscles from DJ-1 KO mice compared to WT **(Figure 4E)**, revealing the presence of a skeletal muscle atrophy phenotype in the absence of DJ-1 protein.

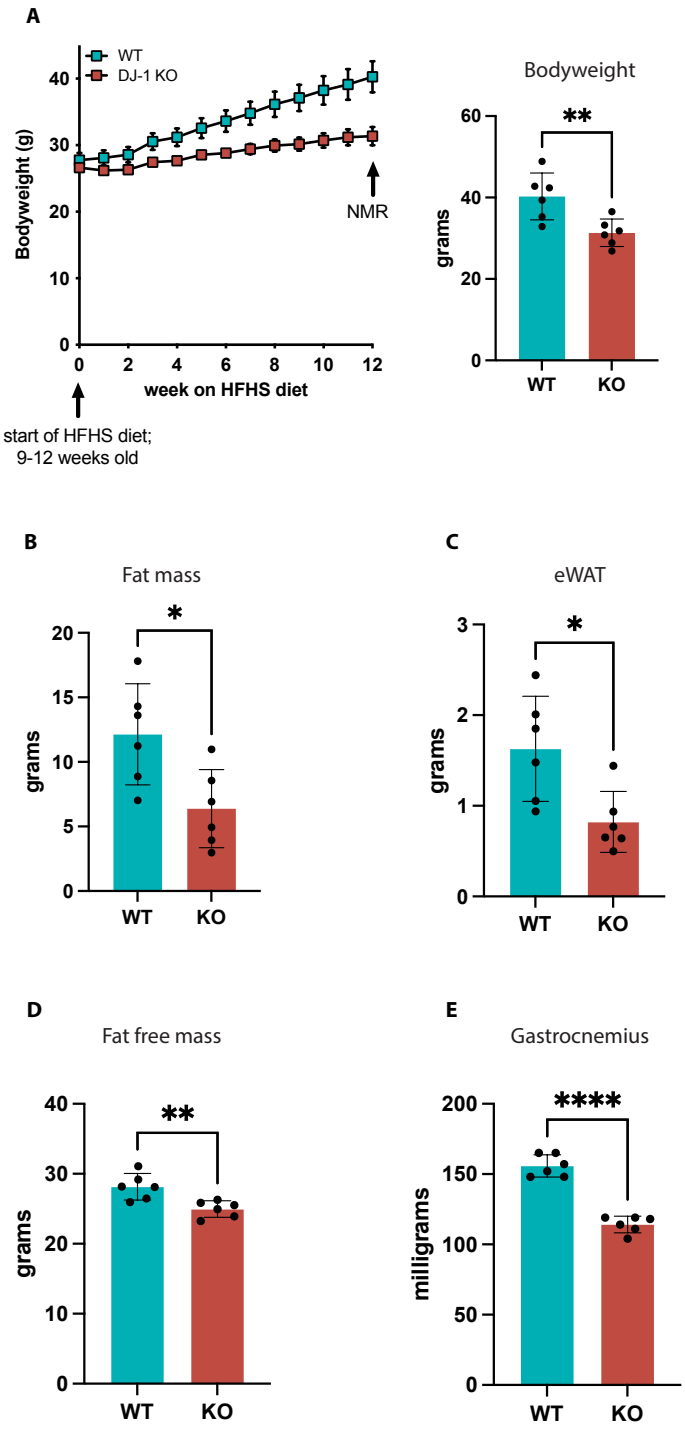

Figure 4. Metabolic phenotyping of DJ-1 KO and WT mice under HFHS diet. (A) bodyweight, (B) fat mass, (C) epididymal white adipose tissue (eWAT) mass, (D) fat free mass, and (E) muscle mass of gastrocnemius from WT and DJ-1 KO mice under high-fat high-sucrose (HFHS) diet. Mean ± sem; n = 6 per group. Statistical analysis performed by unpaired t test. * adj.p ≤ 0.05, ** adj.p ≤ 0.01, **** *adj.p* ≤ 0.0001.

Next, to investigate the possible underlying mechanisms linked to this metabolic phenotype, we used indirect calorimetry analysis to monitor and compare metabolic parameters between both genotypes. Surprisingly, the resistance to the diet-induced weight gain of DJ-1 KO mice on HFHS diet could not be accounted for by changes in either energy expenditure **(Figure 5A)**, daily food intake **(Figure 5B)**, source of utilized fuels **(Figure 5C)**, or locomotor activity **(Figure 5D)**.

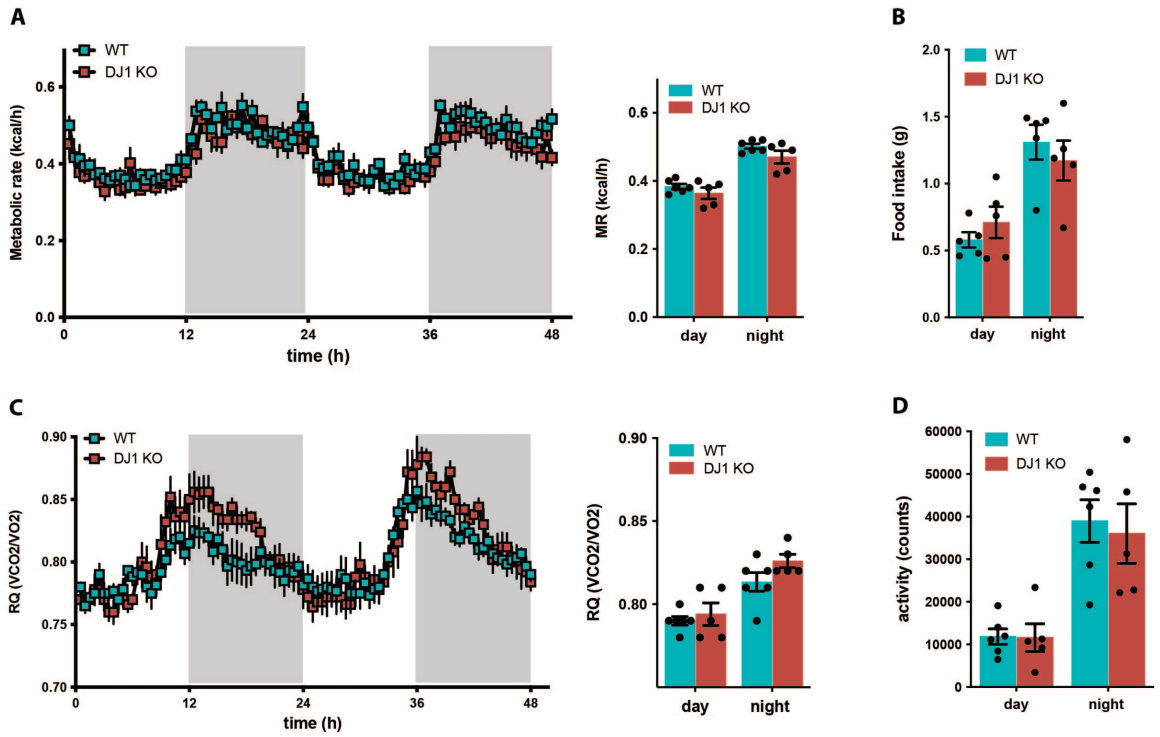

Figure 5. Indirect calorimetry analysis from WT and DJ-1 KO mice under HFHS diet. Measurements from TSE system metabolic cages of (A) Energy expenditure, (B) food intake, (C) respiratory exchange ratio (RER), and (D) locomotor activity of WT and DJ-1 KO mice under HFHS diet. Mean ± SEM; n = 5-6 per group. Statistical analysis performed by two-way ANOVA.

Taken together, our data from metabolic phenotyping of WT and DJ-1 KO male mice under chronic metabolic stress suggested that DJ-1 loss results in intrinsic differences in muscle metabolism, which could be driving the overall changes in the systemic metabolism.

Loss of DJ-1 causes selective atrophy of fast glycolytic type 2B muscle fibers

To further explore the atrophy phenotype, we performed histological analysis of gastrocnemius tissue sections from WT and DJ-1 KO mice under HFHS diet. For that, samples were stained with laminin to outline the individual myofibers and with anti-myosin antibodies specific for type 1 slow (blue), fast type 2A (green), and fast type 2B (red) myosin heavy chains **(Figure 6A)**. Fast type 2X fibers were not stained and appear black. As a result, we identified a decrease in fiber size from DJ-1 KO gastrocnemius muscle compared to control **(Figure 6B, left)**, in agreement with our previous observation of skeletal muscle atrophy phenotype due to DJ-1 loss. More specifically, by analyzing the fiber size according with the fiber type, we observed that the muscle atrophy of KO mice was restricted to the highly glycolytic fast type 2B myofibers **(Figure 6B, right)**, suggesting that DJ-1 expression and function were more related to glycolytic rather than to oxidative metabolism.

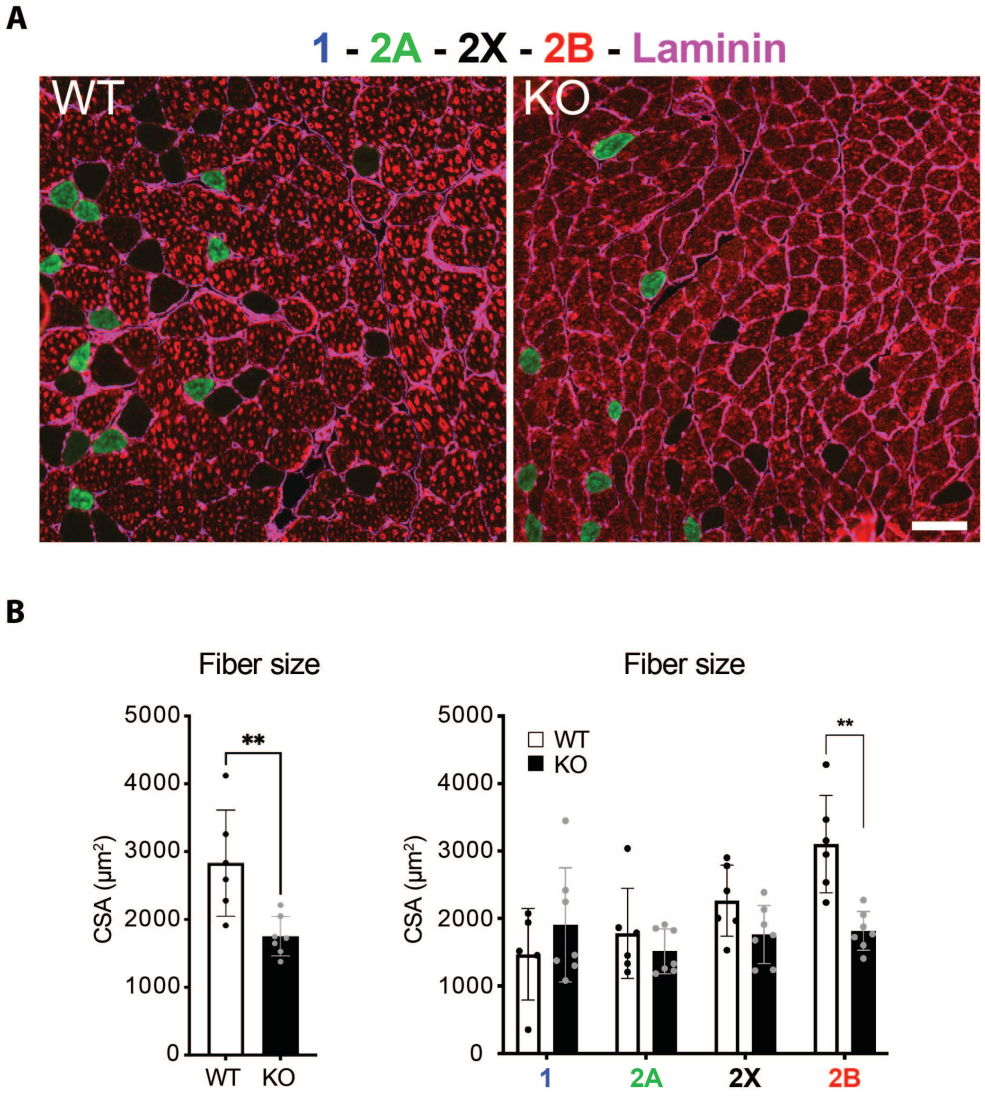

Figure 6. Histological analysis of gastrocnemius muscle from WT and DJ-1 KO. (A) Transverse sections of gastrocnemius from WT and KO mice under HFHS diet stained with anti-myosin antibodies specific for slow type 1 (blue), fast type 2A (green) and fast type 2B (red) myosin heavy chains. Fast type 2X fibers are unstained and appear black. Scale bar is 100 μm. (B) Total fiber size in WT and KO muscles under HFHS diet (left), and fiber size according to fiber type (right). Mean ± SEM; *n* = 6-7 per group. Statistical analysis performed by unpaired t test and unpaired t test with post hoc Holm-Sidak test. ** $p \leq 0.01$. CSA, cross sectional area; 1, type 1 slow (blue); 2A, fast type 2A (green); 2X, fast type 2X fibers (black); and 2B, fast type 2B (red) myosin heavy chains.

Muscle atrophy in DJ-1 KO mice is linked to increased glycation stress

To explore potential molecular signatures in the skeletal muscle linked to DJ-1 loss, we performed untargeted metabolomics by using reversed phase-ultrahigh-performance liquid chromatography-tandem mass spectrometry (RP-UHPLC-MS/MS) in gastrocnemius tissues from WT and DJ-1 KO mice after 12 weeks under HFHS diet **(Figure 7A)**. Interestingly, principal component analysis (PCA) showed a very distinct metabolic separation when comparing both genotypes **(Figure 7B)**. Among approximately 360 detected amino acids, carbohydrates, cofactors, lipids, nucleotides, and peptides, random forest analysis identified 97 genotype-associated metabolites, from which 89 were increased and 8 were decreased in DJ-1 KO muscles **(Figure 7C)**.

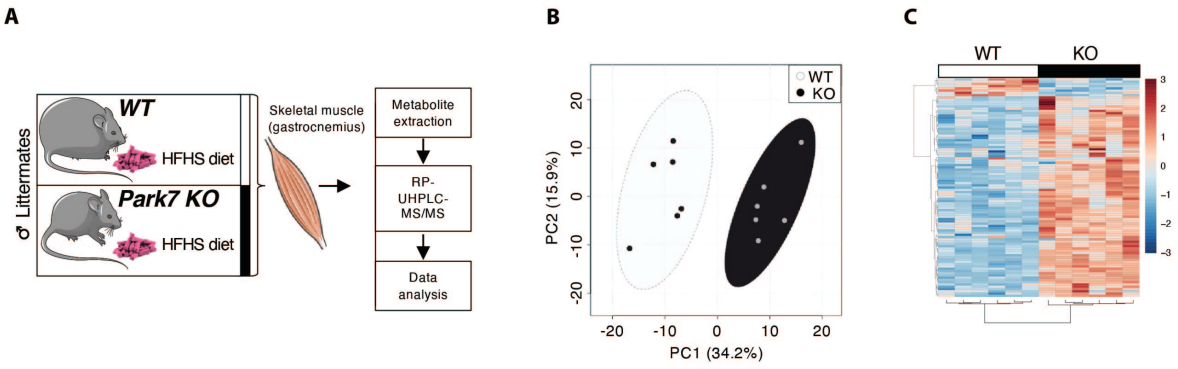

Figure 7. Metabolomics analysis of gastrocnemius from WT and DJ-1 KO under HFHS diet. (A) Scheme of experimental design. Figure elements modified from SMART (Servier Medical Art), licensed under a Creative Common Attribution 3.0 Generic License. **http://smart.servier.com/**. (B) Principal component analysis of the entire metabolomics data set. (C) Heatmap of 97 metabolites selected by random forest shown for individual samples. Scale bar indicates Z-score.

Compared to control, overall untargeted metabolomics analysis showed that skeletal muscle from DJ-1 KO mice had a higher expression of metabolites related to protein degradation **(Figure 8A)**, such as 1-methylhistidine; redox homeostasis **(Figure 8B)**, including S-adenosylmethionine (SAM), spermidine, and glutathione (GSH); as well as arginine (R) and lysine (K) metabolites, such as trimethyllysine (TMK), and carboxymethyllysine (CML), a major AGE **(Figure 8C)**. Together, our

results showed that muscles from DJ-1 KO were under increased glycation stress, oxidative damage, and activation of protein degradation, likely causing the selective atrophy of highly glycolytic type 2B myofibers.

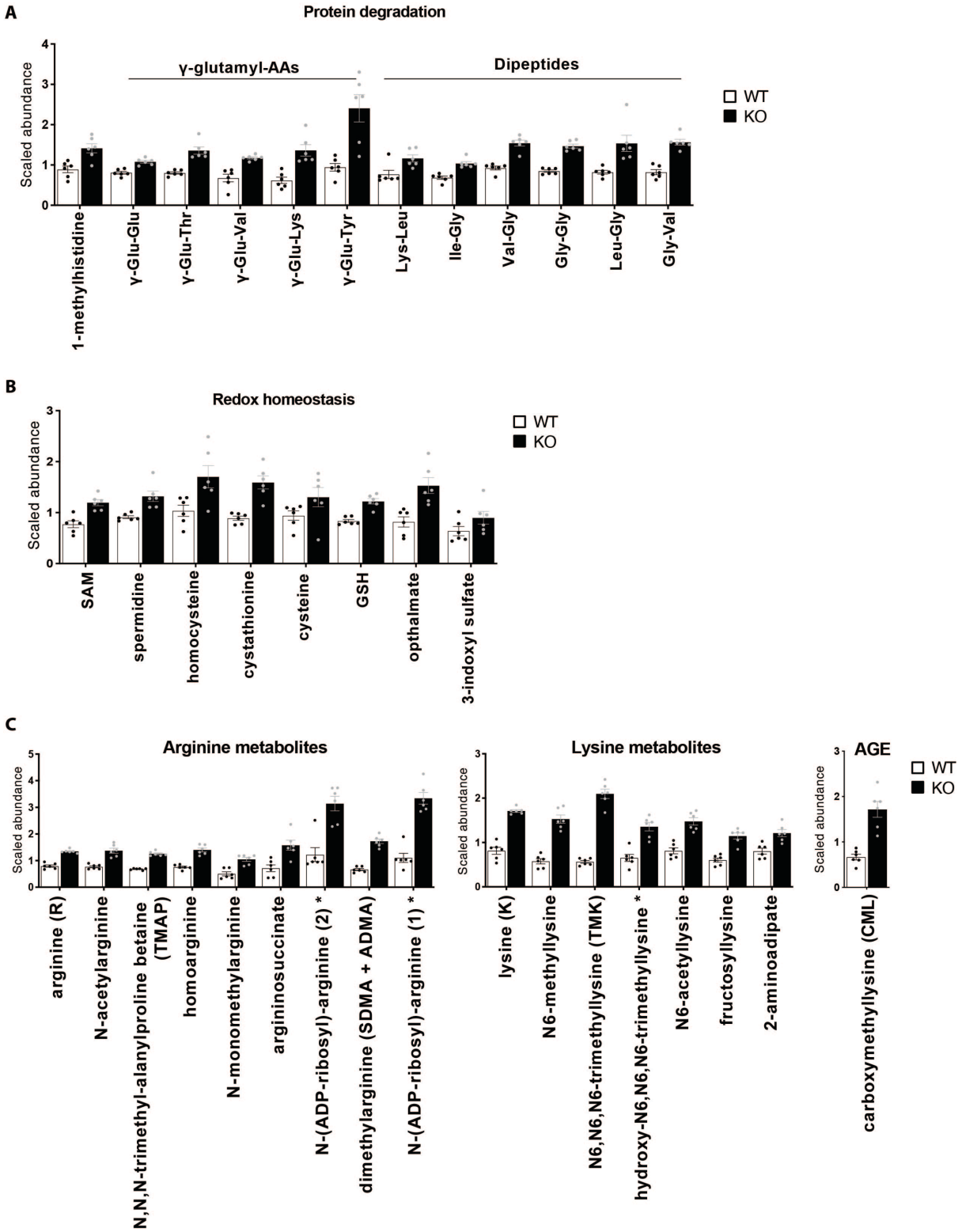

Figure 8. Relative abundance of selected metabolites. Relative abundance of selected groups of metabolites identified by random forest as significantly increased in DJ-1 KO gastrocnemius muscles under HFHS diet. Mean ± SEM; *n* = 6. *Indicates compounds that have not been confirmed based on a standard (i.e. Not Tier 1).

DJ-1 loss leads to specific AGE accumulation in mice skeletal muscle

To further understand to which extent the metabolic signature was diet-dependent, as well as to validate the previous findings, we established a second mouse cohort in which WT and DJ-1 KO mice were under chow or HFHS diet for 12 weeks. To also explore tissue-specificity, we collected plasma and other highly metabolic relevant tissues such as liver and brain to perform a second untargeted metabolomics analysis alongside gastrocnemius samples. This time, to increase the coverage of identified metabolites and include both polar and nonpolar analytes, we chose to use hydrophilic interaction liquid chromatography (HILIC)-tandem MS/MS method **(Figure 9)**.

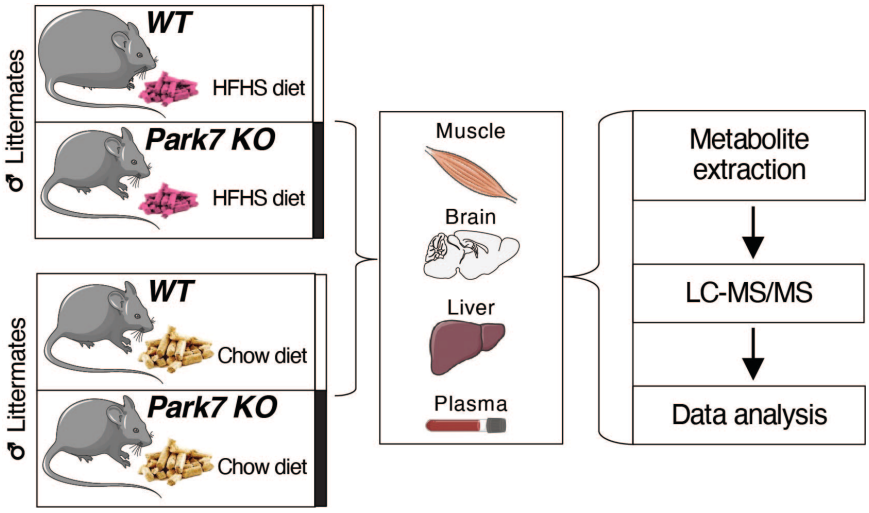

Figure 9. Metabolomics experimental design across different tissues and under different diets. Scheme of experimental design from metabolomics performed in gastrocnemius, brain, liver, and plasma under both HFHS and chow diet. Figure elements modified from SMART (Servier Medical Art), licensed under a Creative Common Attribution 3.0 Generic License. http://smart.servier.com/.

As an initial validation of our previous findings, we could again observe the increased AGEs associated metabolites, such as TMK, lysine (K), and arginine (R), in the skeletal muscle of DJ-1 KO under HFHS diet **(Figure 10A)**. Importantly, these metabolites were also increased under chow diet **(Figure 10B)**, suggesting that AGEs accumulation was linked to DJ-1 loss rather than the diet. Moreover, we found three

unknown metabolites that had a 7-10 foldchange accumulation in DJ-1 KO compared to WT under both diets **(Figure 10)**.

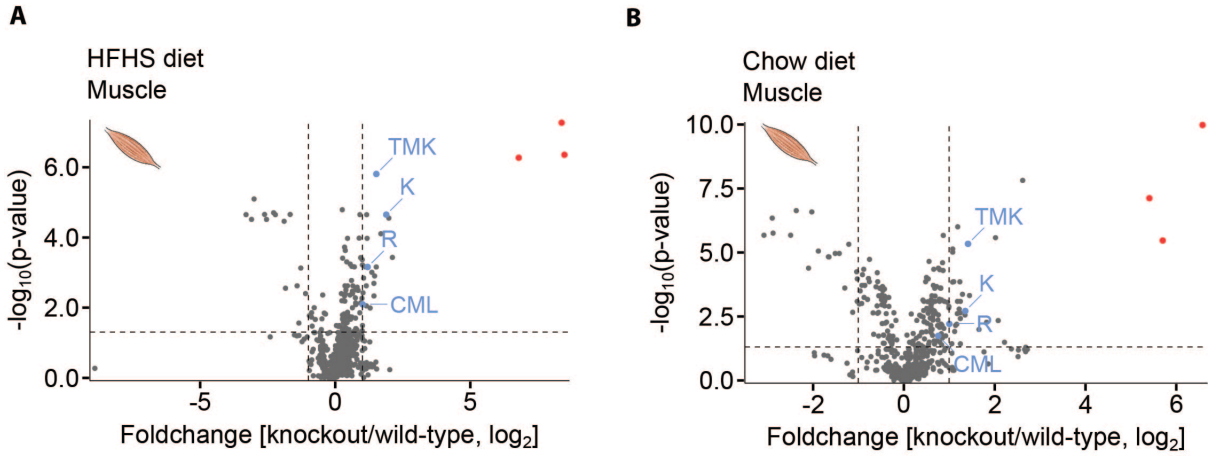

Figure 10. Volcano plots of metabolomes of gastrocnemius muscle from WT and DJ-1 KO mice under different diets. Volcano plots of metabolomes for WT and DJ-1 KO gastrocnemius under (A) high-fat high-sucrose diet (HFHS) and (B) chow diet. Statistical analysis performed by t-test. AGE related metabolites arginine (R), lysine (K), trimethyllysine (TMK), and carboxymethyllysine (CML) are indicated in blue. Unknown identified metabolites are indicated in red.

After intensive analysis of their MS/MS fragmentation pattern, we could predict their chemical structure and identify these so far undescribed metabolites also as AGEs: α-glycerinylarginine (α-GR), α/ε-glycerinyllysine (α/ε-GK), and glycerinyltrimethyllysine (GTMK) **(Figures 11A,B)**.

A

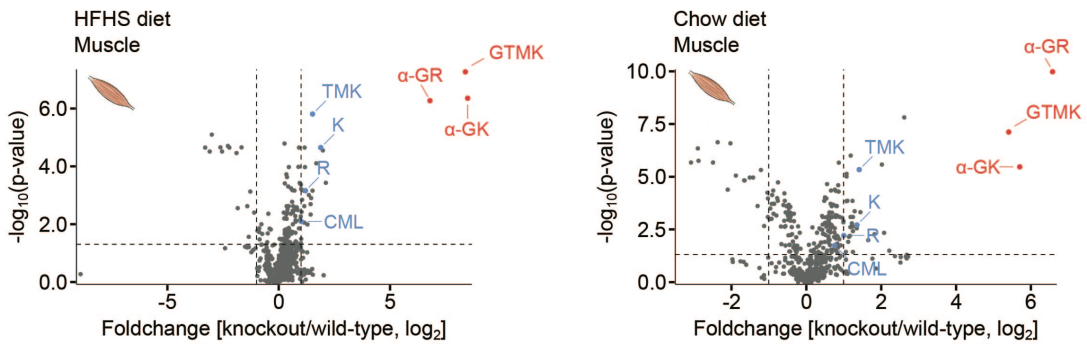

B

α-N-glycerinylarginine (α-GR)

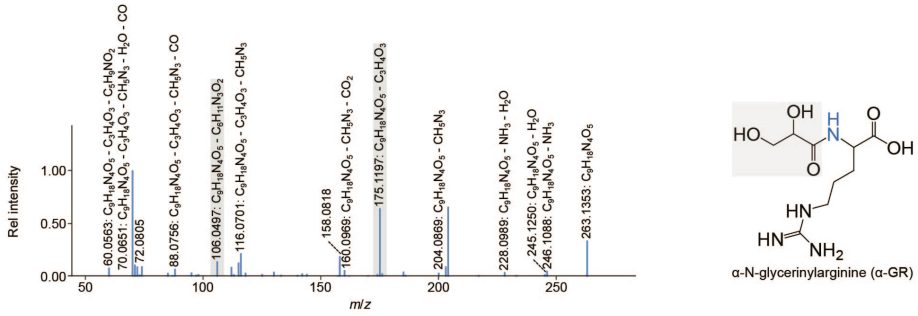

α-N-glycerinyllysine (α-GK)

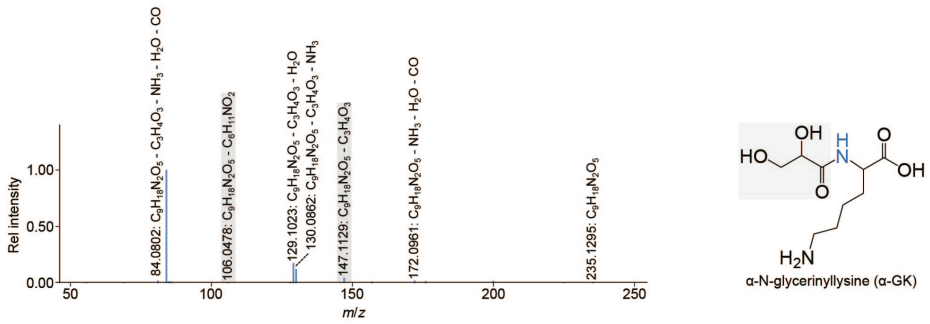

α-N-glycerinyltrimethyllysine (α-GTMK)

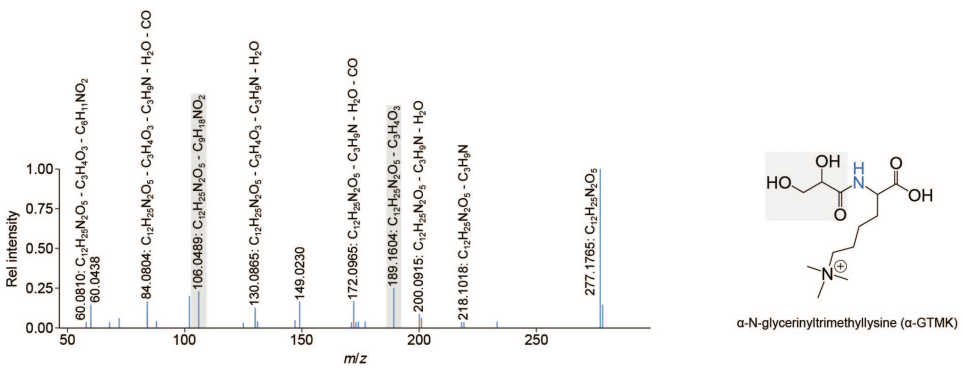

Figure 11. Accumulation of glycerinyl-AGEs in gastrocnemius muscle of DJ-1 KO mice. (A) Volcano plots of METABOLOMES for WT and DJ-1 KO gastrocnemius under HFHS (left) and chow diet (right). Statistical analysis performed by t-test. Glycerinyl-AGEs N-α-glycerinylarginine (α-GR), N-α-glycerinyllysine (α-GK), and N-α-glycerinyltrimethyllysine (α-GTMK) are indicated in red, while related metabolites arginine (R), lysine (K), trimethyllysine (TMK), and carboxymethyllysine (CML) are indicated in blue. (B) MS/MS fragmentation pattern and elucidation of the chemical structures of detected glycerinyl-AGEs.

By exploring a possible tissue-specificity, we noticed that the accumulation of these metabolites, as well as the other previously identified AGEs associate metabolites, were specific to the skeletal muscle of DJ-1 KO mice, as they were not observed in liver, plasma, or brain under neither HFHS **(Figure 12A)** nor chow diet **(Figure 12B)**. Together, our data support the idea of a basic link between AGEs accumulation and DJ-1 loss and reveal the accumulation of three new identified AGEs specifically in the skeletal muscle of DJ-1 KO mice.

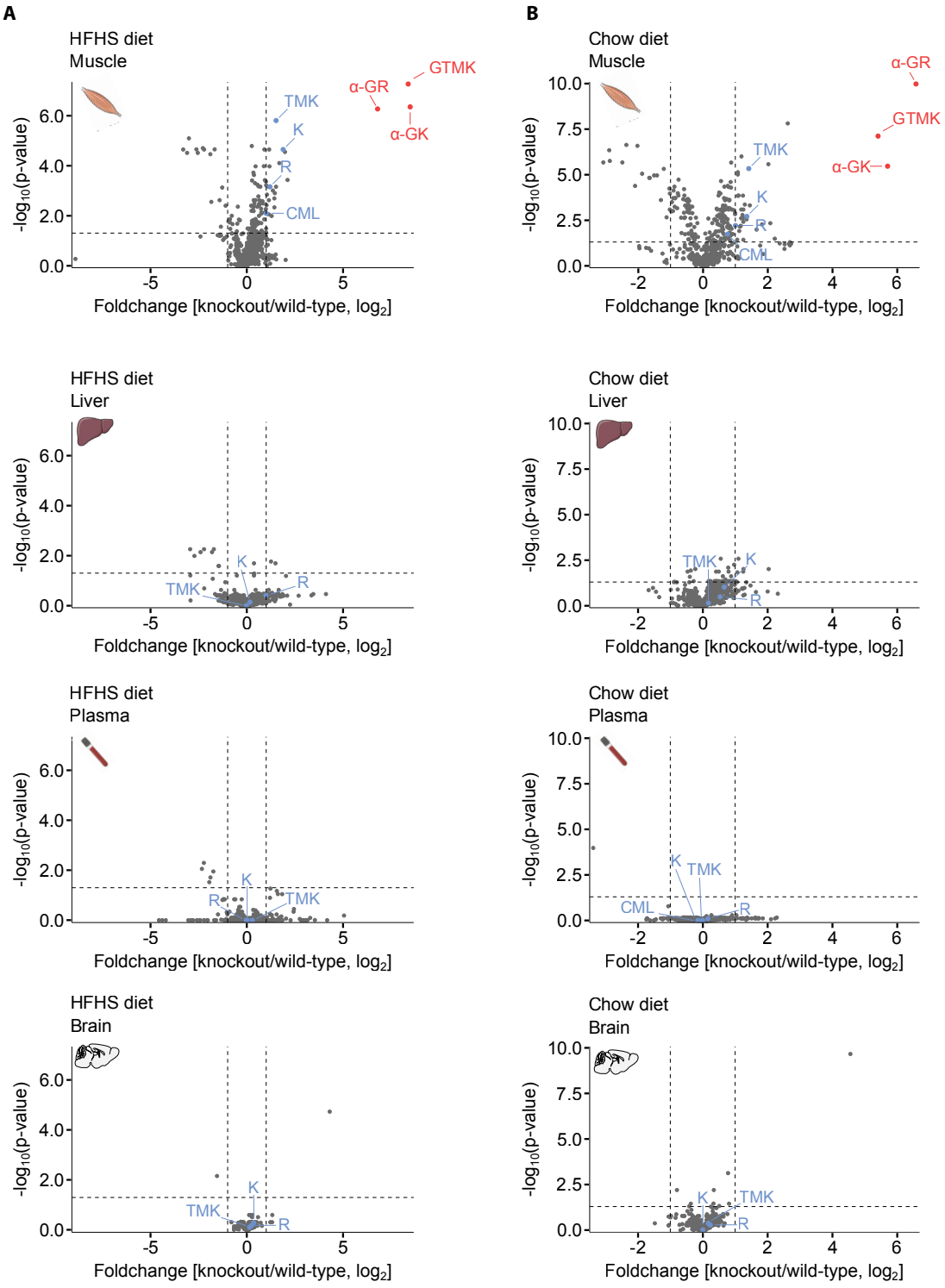

Figure 12. Volcano plots of metabolomes from WT and DJ-1 KO across different tissues and under different diets. Volcano plots of METABOLOMES for WT and DJ-1 KO gastrocnemius, liver, plasma, and brain under (A) high-fat high-sucrose diet (HFHS) and (B) chow diet. Statistical analysis performed by t-test. Glycerinyl-AGEs N-α-glycerinylarginine (α-GR), N-α-glycerinyllysine (α-GK), and N-α-

glycerinyltrimethyllysine (α-GTMK) are indicated in red, while related metabolites arginine (R), lysine (K), trimethyllysine (TMK), carboxymethyllysine (CML) are indicated in blue.

To confirm the chemical structure of the newly identified AGEs, we ordered commercially synthesized authentic α-GR and α-GK chemical standards, as well as the commercially available ε-GK. Unfortunately, due to a challenging chemical synthesis, we could not order a commercially synthesized authentic GTMK standard. Nevertheless, by spiking the chemical standards in the MS together with our samples, we could confirm the initial predicted structure and confirm that the modification was at the α-amino group of the arginine and lysine **(Figures 13A,B)**.

A

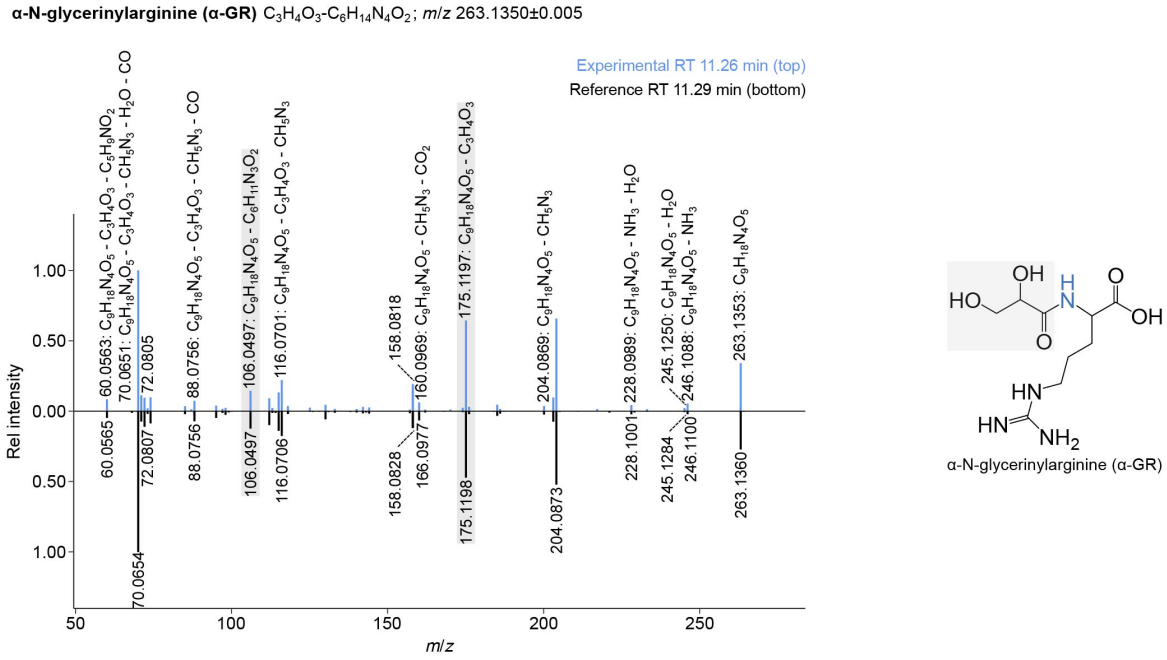

B

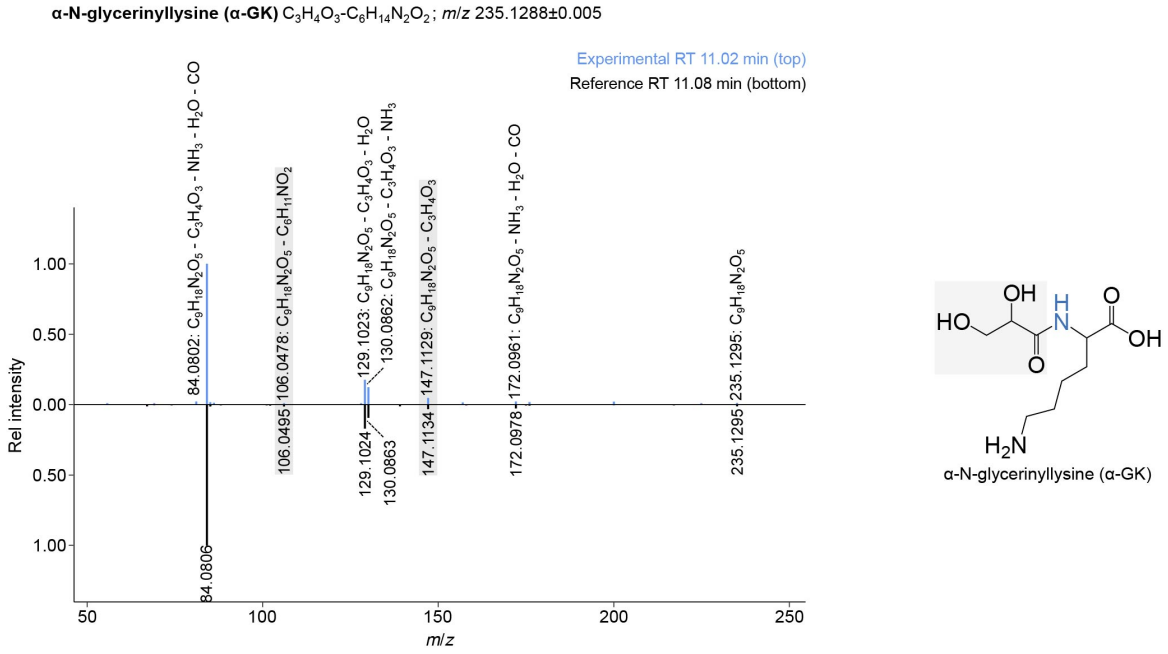

Figure 13. Structural validation of α-GR and α-GK. Additional verification of the glycation sites based on retention time and MS/MS comparison with authentic chemical standards for (A) N-α-glycerinylarginine (α-GR) and (B) N-α-glycerinyllysine

(α-GK). Experimental spectra are shown in blue (top) and reference spectra in black (bottom).

Analysis performed in fibroblasts from Parkinson's disease (PD) patients

Glycerinyl-AGEs α-GR and α-GK are specific biomarkers for PARK7-related early-onset PD

To investigate the translational potential of these newly identified AGEs, we decided to explore the accumulation of these metabolites in samples from Parkinson's disease (PD) patients. For that, we used skin fibroblasts from two Park7-related PD patients, one male and one female, that had different mutations in the Park7 gene and were around 28-29 years old at the time of disease onset (**Figures 14A,B)**.

A

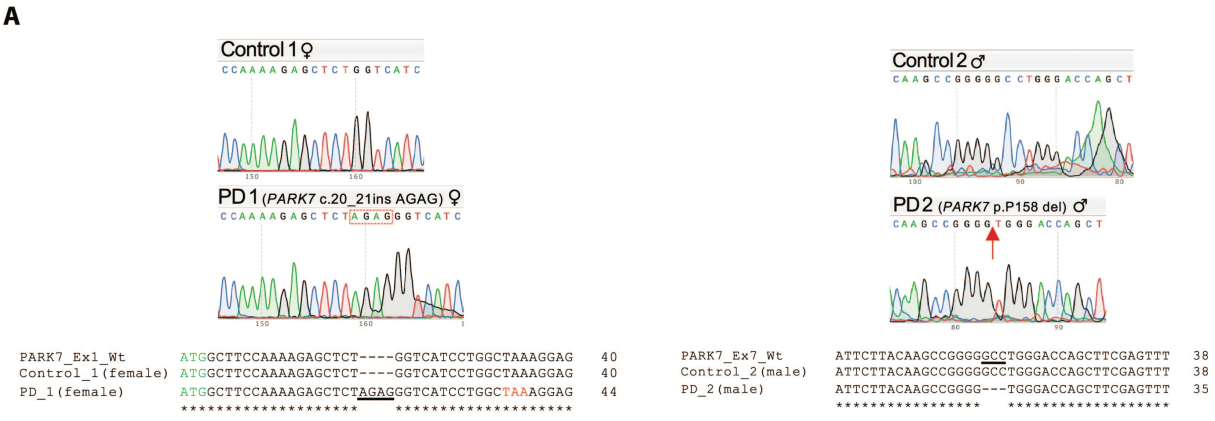

B

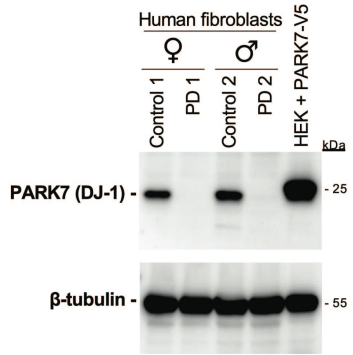

Figure 14. Sequence alignments and confirmation of fibroblast samples from PARK7-related PD patients. (A) Sequence alignments and electropherograms of fibroblast DNA from two *PARK7* variants with respective controls. (Left) Female patient (PD 1) carries a 4bp insertion in exon 1 (c.20_21ins AGAG, indicated by the red dashed box) leading to frameshift and premature stop codon, whereas the female control (control 1) has a wildtype allele at the same position. ATG start codon is indicated by green text; premature stop codon TAA is indicated by red text. (Right) Male patient (PD 2) carries a 3bp loss in exon 7 (p.P158del) indicated by the red arrow, whereas the male control (control 2) has a wildtype allele at the same position. (B) Western blot showing representative PARK7 (DJ-1) protein levels in control and patient fibroblasts. HEK293 cells transfected with V5-tagged *PARK7* cDNA construct were included as a positive control.

Considering possible influences from the in vitro condition in the results, patients' skin fibroblasts were cultured under both high (4.5 g/L) and low (1.0 g/L) glucose medium before harvesting and sending for MS analysis. Based on our results, α-GR, α-GK, and ε-GK were detected in both PD patients' fibroblasts, while they were not detected in any of the control samples **(Figure 15)**, showing that these previously unknown AGEs were also accumulated in Park7-related PD. We did not observe major differences when comparing the high and low glucose conditions.

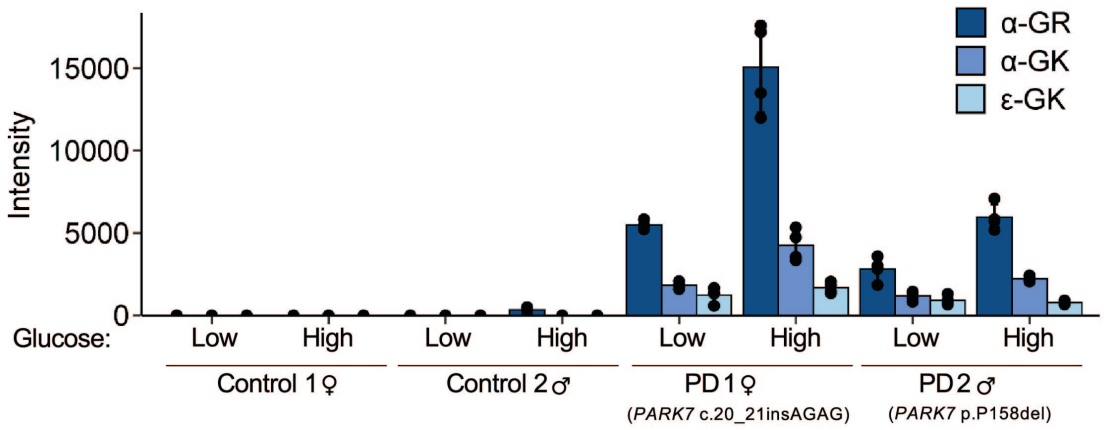

Figure 15. Glycerinyl-AGEs α-GR and α-GK measurement in PARK7-related early-onset PD patient fibroblasts. Glycerinyl-AGEs N-α-glycerinylarginine (α-GR), N-α-glycerinyllysine (α-GK), and N-ε-glycerinyllysine (ε-GK) in fibroblasts from control and *PARK7*-related PD patients cultured under low (1.0 g/L) or high (4.5 g/L) glucose medium. Mean ± SD; *n* = 3.

Next, to start exploring whether the accumulation of these AGEs was specific to PARK7 mutation or had a broader link to PD cases, we repeated the previous experiment with five additional patients' skin fibroblast samples, which included three idiopathic samples and two with mutations in GBA1 (glucosylceramidase beta 1). As a positive control from the previous experiment, we also included the previous two Park7-related PD in the experimental design. This time, however, we performed the experiment only under high glucose medium. After MS measurement and data analysis, we could detect again α-GR, α-GK, and ε-GK in both Park7 PD samples, but not in the other PD samples or their respective controls **(Figure 16)**, reinforcing that the accumulation of these compounds is specific to DJ-1 loss and suggesting that these glycerinyl-AGEs α-GR and α-GK could have potential as specific biomarkers for Park7-related early-onset PD.

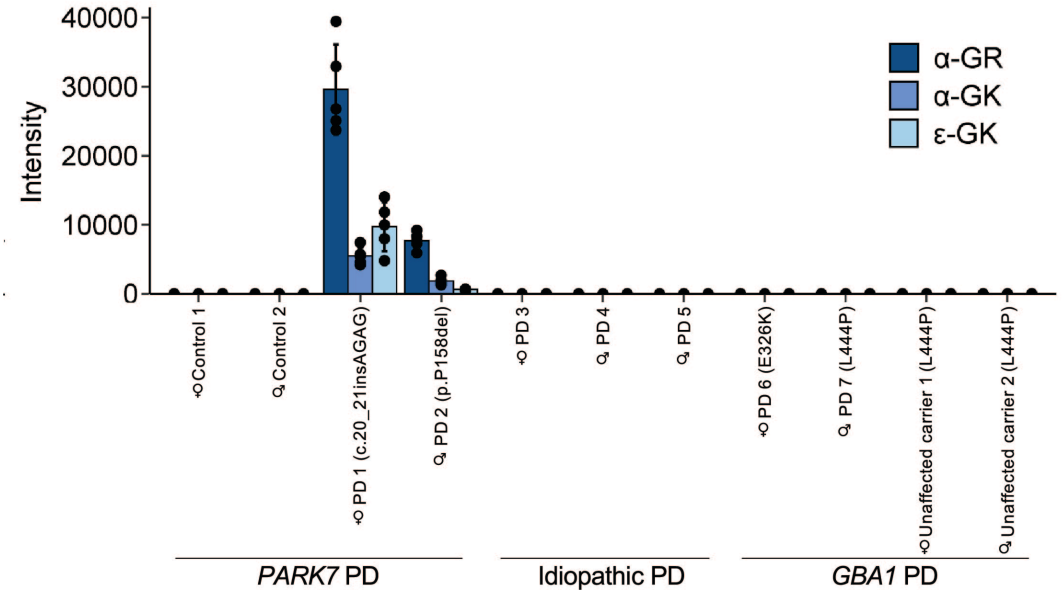

Figure 16. Glycerinyl-AGEs α-GR and α-GK measurement in PD patients' fibroblast samples. Glycerinyl-AGEs in fibroblasts from control and *PARK7*-related, idiopathic, and *GBA1*-related PD patients cultured under high (4.5 g/L) glucose (mean ± SD; *n* = 5). *GBA1*, glucosylceramidase beta 1.

DISCUSSION

Since its discovery in 1997 as a novel oncogene (Nagakubo et al., 1997), DJ-1 protein has shown to be ubiquitously expressed across different tissues and play multifunctional roles, being associated with both overall metabolic changes and PD. Although DJ-1 KO mice do not show the typical age-dependent degeneration of dopaminergic neurons of PD, they exhibit increased susceptibility to a variety of oxidative insults and phenotypic differences that can be induced by chronic metabolic stress (Kim et al., 2014; Shi et al., 2015). In this study, we aimed to further investigate the effects of DJ-1 loss in the systemic metabolism, alongside its potential deglycase activity, since AGEs have been already linked with ageing, diabetes complications, and neurodegenerative diseases. Our results demonstrated in vivo the detrimental effects of DJ-1 loss in skeletal muscle mass, likely driving the resistance to diet-induced weight gain, and in AGEs detoxification. Interestingly, AGEs were accumulated specifically in the skeletal muscle from DJ-1 KO mice, under either chow or HFHS diet, indicating a basic link between DJ-1 loss and AGEs accumulation. Moreover, our metabolomics analysis allowed us to identify three new AGEs structures, which were also accumulated in skin fibroblasts from Park7-related PD patients, showing that this DJ-1 function associated with AGEs formation is also preserved in humans.

Regarding the metabolic phenotyping of DJ-1 male mice, our results showed that DJ-1 deficiency mitigated the expected HFHS diet-induced weight gain **(Figure 4A),** significantly reducing fat mass **(Figures 4B)**, eWAT accumulation **(Figures 4C)**, and fat free mass **(Figures 4D)**. Although this resistance to diet-induced obesity (DIO) was not observed in the male mice, a previous study using high-fat diet (HFD) reported a similar phenotype in female DJ-1 KO mice (Shi et al., 2015). In this study, authors reported an increased oxygen consumption in female mice associated with a higher energy expenditure, claiming that the maintenance of cellular metabolic homeostasis by DJ-1 in the murine skeletal muscle is linked to modulation of ROS levels (Shi et al., 2015). However, in accordance with their data from male mice, our analysis from metabolic cages also showed no differences in energy expenditure **(Figures 5A)**, food intake **(Figures 5B)**, RER **(Figures 5C)**, and activity **(Figures 5D)** between WT and DJ-1 KO male mice, pointing out to possible sex differences in the interplay between DJ-1 and metabolism. Moreover, our observations of decreased fat free mass **(Figure**

4D) together with the skeletal muscle atrophy phenotype **(Figure 4E)** clearly indicate a detrimental rather than beneficial effect of DJ-1 loss under chronic metabolic stress.

Our results clearly support that DJ-1 deficiency results in resistance to diet-induced obesity, as previously reported (Shi et al., 2015). However, this phenotype is still conflicting with the literature as other studies did not observe significant differences in the BW when comparing WT and DJ-1 KO after 12-14 weeks of HFD intervention (Kim et al., 2014; Seyfarth et al., 2015). This discrepancy in results could be, for example, due to differences in the DJ-1 KO model that was used, i.e. deletion of exons 3-5 (Shi et al., 2015) or gene trap inserted between exon 6-7 (Kim et al., 2014; Seyfarth et al., 2015), which was similar to the one used in our study; or in the composition of the diet used, for example between HFHS or HFD (Kim et al., 2014; Seyfarth et al., 2015; Shi et al., 2015). Nevertheless, all studies showed that DJ-1 interplays with metabolism, especially in high metabolic tissues such as liver, adipose tissue, and skeletal muscle.

Here, our data suggested that intrinsic changes in the skeletal muscle could be driving the resistance to diet-induced weight gain. Importantly, weight loss and sarcopenia, an excessive loss of skeletal muscle mass and muscle strength, have become a progressive public health concern among some chronic disease patients. However, although DJ-1 protein has shown a clear importance for the overall and the skeletal muscle metabolism, the association among loss of skeletal muscle mass, nutritional overload, and neurodegenerative diseases remain to be further addressed, likely due to the complexity of these multifactorial systems. Additional studies trying to rescue this metabolic phenotype with re-expression of DJ-1 specifically in the skeletal muscle will bring valuable information to the literature. Moreover, evaluating the progression of the metabolic changes at different time points would also contribute to have a better understanding of the possible underlying mechanisms associated between alterations in skeletal muscle metabolism and overall bodyweight and fat mass accumulation, which could for example contribute for drug development for cancer cachexia, diabetes, obesity, and neurodegenerative and neuromuscular diseases.

Our results showed that global DJ-1 loss resulted in a selective decrease of fiber size from the highly glycolytic fast type 2B myofibers **(Figure 6)**, leading to reduced gastrocnemius mass **(Figure 4E)**. These fast glycolytic type 2B fibers present high

glycolytic rates and increased reliance on anaerobic adenosine triphosphate (ATP) production compared to more oxidative fast type 2X, 2A and slow type 1 myofibers (Smith et al., 2023), being considered the ones with the highest mechanical energy produced per unit of time among rodents (Schiaffino & Reggiani, 2011). Interestingly, previous study has also shown that skeletal muscle from DJ-1 KO mice have increased expression of mRNA levels of genes associated with glycolysis when compared to control (Shi et al., 2015), suggesting that DJ-1 have an important role associated to glycolysis metabolism. Together, our results from skeletal muscle analysis suggested that DJ-1 is more related to glycolytic rather than oxidative metabolism. However, further investigation such as data integration of single fiber proteomics and metabolomics analysis from DJ-1 KO skeletal muscle can contribute for better understanding the importance and the mechanisms associated with DJ-1 functions in glycolytic and oxidative metabolisms.

According to our whole tissue metabolomics analysis, skeletal muscle from DJ-1 KO mice showed higher glycolytic by-products alongside markers of protein degradation and glycation oxidative stress **(Figures 7,8)**. The increased levels of TMK, fructosyllysine and CML, a major AGE, indicated that AGEs accumulation could be related to the observed skeletal muscle atrophy phenotype. Indeed, AGEs formation, an important example of glycation reaction, have already been associated with skeletal muscle atrophy, and was recognized as a risk factor for lowering motor function and muscle function (Yabuuchi et al., 2020). Its accumulation has been linked with muscle wasting in mouse and human myoblast, where it seems to reduce myotube diameter and negatively regulate myogenesis, and with muscle atrophy and muscle dysfunction in diabetic skeletal muscles of mice and patients (Chiu et al., 2016). Interestingly, a fiber type shift towards a faster profile in soleus skeletal muscle from diabetic mice without insulin treatment was suggested to decrease insulin sensitivity in this muscle and to increase AGE accumulation (Snow et al., 2009), indicating a possible correlation among fiber type composition, insulin sensitivity and AGEs accumulation. Likewise, DJ-1 deficiency was also reported to promote a similar shift in fiber type in soleus skeletal muscle, inducing an adaptation to enhance glycolytic capacity (Shi et al., 2015). Based on our metabolomics results, the absence of DJ-1 leads to higher glycolytic by-products and AGEs accumulation in gastrocnemius skeletal muscle, a fast-twitch type muscle with a mix of type I, IIA and IIB fibers, suggesting an increase in glycolysis and consequently in glycating events. However, further analysis is needed

to understand whether DJ-1 directly regulates glycolysis or also promotes a shift from oxidative to glycolytic fibers in gastrocnemius muscle when absent. Experiments comparing metabolomics analysis between soleus and extensor digitorum longus (EDL) muscles from DJ-1 KO mice, as well as their fiber type composition, will contribute to clarify how DJ-1 loss leads to increased glycolysis.

Our finding of AGEs accumulation in skeletal muscles from DJ-1 KO mice under both chow and HFHS diet **(Figure 10)** indicated a genotype rather than diet-dependent association. This result is supported by recent studies in Escherichia coli that proposed DJ-1 and its protein family to function as protein deglycases (Advedissian et al., 2016; Richarme et al., 2015), repairing cysteines, arginines and lysines from glycation by glyoxal and methylglyoxal, and thus playing an important role in preventing protein glycation and in the process of AGEs clearance (Advedissian et al., 2016). However, as mentioned before, whether DJ-1 shows deglycase activity is a current topic of debate (Andreeva et al., 2019; Mazza et al., 2022; Pfaff et al., 2017b, 2017a; Richarme, 2017; Richarme et al., 2015; Richarme & Dairou, 2017). Contradictory work has suggested that DJ-1 instead functions as a minor glyoxalase (Choi et al., 2023; Gao et al., 2023; Lee et al., 2012), detoxifying the potent glycating agent methylglyoxal through its conversion into lactate rather than repairing glycation damage on proteins. Most recently, DJ-1 was proposed to act as a detoxification enzyme for 1,3-bisphosphoglycerate, a reactive glycolytic intermediate formed spontaneously that avidly reacts with amino groups (Heremans et al., 2022), claiming that DJ-1 prevents damage caused by a metabolite from glycolysis. Nevertheless, although the latter supports our hypothesis for a specific protection function of DJ-1 related to glycolysis, the identification of increased levels of glycerinyl-modified arginine and lysine metabolites (α-GR, α-GK, and α-GTMK), of the common Amadori products fructosyllysine, and of the major AGE species CML in atrophic muscles from DJ-1 KO mice in our data **(Figure 11)** corroborates with the potential deglycase activity for DJ-1. Together, these competing theories point not only to a clear relationship between DJ-1 and glycotoxins, but also to the need for taking differences among models and tissues into further consideration to understand the DJ-1 detoxification role of AGEs under health and pathological conditions.

Interestingly, compared to plasma and other tissues such as brain and liver, our results showed that the accumulation of these three new identified metabolites were

specific to the murine skeletal muscle, both under HFHS **(Figure 12A)** or chow diet **(Figure 12B)**. We believe that due to high dependence on glucose metabolism and relatively high rates of glycolysis in mouse glycolytic muscles (Schiaffino & Reggiani, 2011; Smith et al., 2023), the occurrence of non-enzymatic glycation in this site may be greater than in other cell types, and thus the effects of DJ-1 loss more apparent. Moreover, circulating AGEs, especially in plasma, do not necessary represent the amount of AGEs formation as the accumulation of AGEs in blood is also influenced by liver metabolism and clearance of the kidney, and fluctuate over time (Miyata et al., 1997; Sebeková et al., 2002; Yagmur et al., 2006). However, our results contrast with a recent study that showed accumulation of a broad range of glycerinyl- and phosphoglycyrinyl-modified proteins and amino acids in PARK7 knockout cell lines and mouse brains (Heremans et al., 2022), including glutamate, glutathione, glutamine, glycerophosphoethanolamine, and lysine, which was modified only at the ε-amino group. Differences in detection could be due to analytical considerations, like variances in sample preparation (protein precipitation vs. liquid-liquid extraction), separation technique (HILIC vs. RP), and MS mode (positive vs. negative ionization), which can all lead to recognizable selectivity for glycerinyl-modified compound detection and should be carefully considered. Thus, our results also underscore the importance of aligning analytical methods with proper biological context for successful identification of clinically relevant molecular signatures.

Based on the structure of the new identified AGEs, our data indicated that α-GR and α-GK **(Figure 13)** may originate from modifications and subsequent degradation of N-terminal arginine and lysine residues in muscle proteins or reaction with free amino acids to form ‘glycation free adducts’ (Rabbani et al., 2016), thus supporting a protective role of DJ-1 in the first stages of glycation (Salahuddin et al., 2014). In proteins, only N-terminal amino acids contain a free α-amino group accessible for potential modification, therefore each detected N-α-glycerinyl-AGE requires a protein with the corresponding amino acid at its N-terminus to be modified and degraded. Indeed, protein glycation is known to occur predominantly on N-terminal residues in biological systems (Rabbani et al., 2016). Interestingly, *in vivo* turnover of most proteins is regulated by the N-end rule (Varshavsky, 2011), and approximately 25% of skeletal muscle proteins are known to undergo covalent N-terminal arginylation prior to their degradation, either by the ubiquitin-proteasome system (Solomon et al., 1998) or by macroautophagy (Yoo et al., 2018). Moreover, besides protein N-termini, arginine

and lysine side chains are known to be especially prone to modification via glycation reactions (Rabbani et al., 2016). Thus, the elucidated structures proposed for the three new identified AGEs, besides high confidence confirmation, are in accordance with the literature and biological functions.

Our results from DJ-1 KO mice supports a DJ-1 deglycase activity and reveals an important protection function related to skeletal muscle atrophy, likely due to AGEs accumulation. Importantly, AGEs association with muscle atrophy was suggested to occur through AGE receptor (RAGE)-mediated AMPK-down-regulation of the Akt signaling pathway (Chiu et al., 2016). Interestingly, RAGE KO mice were also found to be resistant to HFD-induced obesity and insulin resistance, despite the normal food intake (Monden et al., 2013; Song et al., 2014). However, although we aimed to further explore the mechanisms through which AGE could be exerting their biological effect, we were not able to detect RAGE expression even in WT skeletal muscle, neither by western blot nor qPCR (data not shown). Importantly, the antibody worked in lung samples that were used as a positive control, as was suggested by the manufacturer. This initial apparent limitation could be due to RAGE being expressed in skeletal muscle only during muscle development and under stress conditions, as previously reported. Based on that, we could hypothesize that AGE may be acting through another AGE receptor or directly through their cross-link with proteins, which alters their structure and functions. Nevertheless, further investigation is still necessary to better understand the underlying mechanisms linked to skeletal muscle damage and AGE accumulation and to contribute to the development of future target treatments. As an example, Ala-Cl, a thiazolium derivative that cleaves preformed AGEs and breaks crosslinks, demonstrated to be a potential therapeutic candidate to effectively improve diabetic myopathy, muscle atrophy and muscle regenerative capacity by reducing AGEs accumulation (Chiu et al., 2016).

It is well known that AGEs have already been linked with neurodegenerative diseases such as PD. As mentioned before, pathological hallmarks of PD, including PARK7-linked early-onset PD cases (Narendra et al., 2019; Taipa et al., 2016), involve neuronal aggregation of misfolded α-synuclein into insoluble Lewy bodies and progressive degeneration of dopaminergic neurons, especially of the substantia nigra and locus coeruleus. While the exact cause of PD is not yet fully understood, non-enzymatic glycation of proteins is known to stimulate their aggregation, including α-

synuclein (Atieh et al., 2021; Vicente Miranda et al., 2017). Likewise, PARK7 has been implicated in reducing the aggregation of glycated α-synuclein (Atieh et al., 2021; N. Sharma et al., 2019), supporting the notion that glycation stress is a potential pathophysiological trigger for PD, and many other age-associated neurodegenerative diseases (S. Schmidt et al., 2022; Vicente Miranda & Outeiro, 2010). However, due to the limitation of the DJ-1 KO animal model, as well as PINK1 and parkin, regarding the lack of nigrostriatal pathology (Dawson et al., 2010), it is necessary for further studies to use other models such as in vitro dopaminergic cells to understand the effects of AGE in neurodegeneration of this cell population and consequently its link to PD pathology.

By using fibroblast samples from patients with different PARK7 mutation **(Figure 14)**, our analysis was able to detect the accumulation of the new AGEs α-GR and α-GK in skin fibroblasts from both Park7-related PD patients in comparison to their health controls **(Figure 15)**. However, different from a previous study (A. Sharma et al., 2020), we could not observe any difference between the male and the female patients. Yet, a higher sample size is needed to further explore possible sex differences related to the accumulation of these compounds. Furthermore, these metabolites were not detected in other sporadic forms of PD or GBA1-related PD **(Figure 16)**, corroborating with a specificity between the accumulation of these metabolites and PARK7-related cases. Taken together, our results show how loss of PARK7 can manifest differently when comparing mice and human patients, and even lead to heterogeneous clinical profile among different PARK7-related early-onset PD patients, as neither PARK7-related PD patient reported any clinically relevant muscle problems, and while PD 1 reported cataracts (likewise reported in her affected sibling), PD 2 reported no vision problems. Equally important, it also shows how valuable the tool of using animal model studies can be for detecting possible biomarkers and advancing the understanding of the pathophysiology from neurodegenerative diseases. However, more studies with a higher patient sample size are necessary to further explore the specificity and applicability of these molecules as biomarkers.

Previous studies reported that patients at risk for developing PD showed increased plasma oxidative stress along with significantly reduced lymphocyte PARK7 expression (Katunina et al., 2023), suggesting that α-GR and α-GK may be useful biomarkers to already identify at-risk patients before neurological symptoms arise. It

remains to be clarified whether they can be used to monitor disease onset and progression in pre-symptomatic or early-stage PD, or effects of therapeutics in PARK7-related PD patients. Importantly, although PARK7 mutations are rare and account for less than 1% of early-onset PD cases (Taipa et al., 2016), its function can be lost even in individuals without mutations, for example by oxidative stress and aging (Heremans et al., 2022; Meulener et al., 2006). Thus, it will also be important to clarify whether α-GR and α-GK can discriminate between PARK7 deficiency and other glyoxylase deficiencies (Vander Jagt & Hunsaker, 2003). Further studies, including measurements of other relevant cell types like neurons and glial cells (Lind-Holm Mogensen et al., 2023), samples from related monogenic (Imberechts et al., 2022) and broader profiling of sporadic forms of PD, along with investigations of less invasive matrices like urine, are needed to clarify the full extent of their diagnostic potential.

Similar to more established biomarkers, like glycated hemoglobin (Makita et al., 1992) and other glycated plasma proteins (Greifenhagen et al., 2016), α-GR and α-GK could also become general indicators for glycation and carbonyl stress in aging and a range of age-associated metabolic (diabetes, renal failure, cardiovascular disease) and neurodegenerative diseases (Pamplona et al., 2008; Rabbani & Thornalley, 2012). These non-enzymatic glycations are sometimes increased in diabetes mellitus patients (Ahmed & Thornalley, 2007) as a consequence of poorly control of blood glucose levels, and high hemoglobin glycated levels are well known to be associated with diabetes complications, including for example muscle atrophy and cataract formation (Stevens, 1998).

CONCLUSION

DJ-1 protein has shown to play important roles both in metabolism and PD, which are known to have oxidative stress as a common denominator. More than that, DJ-1 is a multifunctional anti-oxidative stress protein that has been proposed to act as deglycase, avoiding the detrimental accumulation of AGEs. It is well known that the formation of AGEs occurs through non-enzymatic modifications of proteins or lipids after exposure to glycating agents such as free reducing sugars (glucose, fructose, and ribose) and methylglyoxal (MGO), with the latter arising as glycolytic by-products and being responsible for approximately 65% of cellular glycation events together with glyoxal (Advedissian et al., 2016; de Vos et al., 2016; Kalapos, 2013; Luevano-Contreras & Chapman-Novakofski, 2010; Thornalley et al., 1999; Maillard 1912). Interestingly, our results showed that DJ-1 loss leads to AGE accumulation in the skeletal muscle, likely causing the observed selective atrophy in the fast glycolytic type 2B fibers, supporting the idea of a protective function associated with glycolysis and glycation in this highly glycolytic site. Moreover, our results also suggested that these intrinsic changes in the skeletal muscle could be driving the observed resistance to diet-induced obesity.

Taken together, our study sheds light on a higher physiological relevance of DJ-1 protein in the murine skeletal muscle and human fibroblasts, likely associated with glycolysis. Moreover, it further supports its role as a deglycase, as we could identify a genotype-dependent AGE accumulation both in mouse and human samples, alongside three new AGEs (α-GR, α-GK, and α-GTMK), which to the best of our knowledge have not been described so far. Here, we showed that this DJ-1 function associated with AGEs accumulation in highly glycolytic tissues was preserved from mouse to human, and we present a-GR and a-GK as potential candidates for future biomarkers for Park7-related PD cases, which could have value in the future for clinical advancements. Moreover, our approach also highlights the importance of understanding the limitations of disease models and of complementing the physiological differences from both animal and patient samples to better understand the relevant functions of an important, ubiquitous and multifunction protein such as DJ-1 for translational studies.

In brief, we performed a systematic and untargeted metabolomics analysis across different metabolic active tissues and under different diets to have a better

overview of the effects of DJ-1 loss in the metabolism and AGEs formation. Our results contributed to the advancement of DJ-1 physiology knowledge, as well as identified and elucidated the structures of new AGEs accumulated also in PARK7-PD patients' fibroblast samples. As it is well known, the pathophysiology of neurodegenerative diseases, as well as metabolic syndromes, are part of a complex mechanism system that still needs to be further explored for the advancement of knowledge and therapeutic treatments. More studies will contribute to the advancement of our work, including in vitro studies investigating the role of AGEs in dopaminergic neurodegeneration, and whether these AGEs are also present in other diseases, such as diabetes and neuromuscular diseases.

REFERENCES

Advedissian, T., Deshayes, F., Poirier, F., Viguier, M., & Richarme, G. (2016). The Parkinsonism-associated protein DJ-1/Park7 prevents glycation damage in human keratinocyte. *Biochemical and Biophysical Research Communications*, *473*(1), 87–91. https://doi.org/10.1016/j.bbrc.2016.03.056

Ahmed, N., & Thornalley, P. J. (2007). Advanced glycation endproducts: What is their relevance to diabetic complications? *Diabetes, Obesity & Metabolism*, *9*(3), 233–245. https://doi.org/10.1111/j.1463-1326.2006.00595.x

Aleyasin, H., Rousseaux, M. W. C., Phillips, M., Kim, R. H., Bland, R. J., Callaghan, S., Slack, R. S., During, M. J., Mak, T. W., & Park, D. S. (2007). The Parkinson's disease gene DJ-1 is also a key regulator of stroke-induced damage. *Proceedings of the National Academy of Sciences*, *104*(47), 18748–18753. https://doi.org/10.1073/pnas.0709379104

Andreeva, A., Bekkhozhin, Z., Omertassova, N., Baizhumanov, T., Yeltay, G., Akhmetali, M., Toibazar, D., & Utepbergenov, D. (2019). The apparent deglycase activity of DJ-1 results from the conversion of free methylglyoxal present in fast equilibrium with hemithioacetals and hemiaminals. *The Journal of Biological Chemistry*, *294*(49), 18863–18872. https://doi.org/10.1074/jbc.RA119.011237

Ariga, H., Takahashi-Niki, K., Kato, I., Maita, H., Niki, T., & Iguchi-Ariga, S. M. M. (2013). Neuroprotective Function of DJ-1 in Parkinson's Disease. *Oxidative Medicine and Cellular Longevity*, *2013*, 683920. https://doi.org/10.1155/2013/683920

Artati, A., Prehn, C., Lutter, D., & Dyar, K. A. (2022). Untargeted and Targeted Circadian Metabolomics Using Liquid Chromatography-Tandem Mass Spectrometry (LC-MS/MS) and Flow Injection-Electrospray Ionization-Tandem

Mass Spectrometry (FIA-ESI-MS/MS). *Methods in Molecular Biology (Clifton, N.J.)*, *2482*, 311–327. https://doi.org/10.1007/978-1-0716-2249-0_21

Ascherio, A., & Schwarzschild, M. A. (2016). The epidemiology of Parkinson's disease: Risk factors and prevention. *The Lancet. Neurology*, *15*(12), 1257–1272. https://doi.org/10.1016/S1474-4422(16)30230-7

Atieh, T. B., Roth, J., Yang, X., Hoop, C. L., & Baum, J. (2021). DJ-1 Acts as a Scavenger of α-Synuclein Oligomers and Restores Monomeric Glycated α-Synuclein. *Biomolecules*, *11*(10), 1466. https://doi.org/10.3390/biom11101466

Aviles-Olmos, I., Limousin, P., Lees, A., & Foltynie, T. (2013). Parkinson's disease, insulin resistance and novel agents of neuroprotection. *Brain*, *136*(2), 374–384. https://doi.org/10.1093/brain/aws009

Baldereschi, M., Di Carlo, A., Rocca, W. A., Vanni, P., Maggi, S., Perissinotto, E., Grigoletto, F., Amaducci, L., & Inzitari, D. (2000). Parkinson's disease and parkinsonism in a longitudinal study: Two-fold higher incidence in men. ILSA Working Group. Italian Longitudinal Study on Aging. *Neurology*, *55*(9), 1358–1363. https://doi.org/10.1212/wnl.55.9.1358

Bandopadhyay, R., Kingsbury, A. E., Cookson, M. R., Reid, A. R., Evans, I. M., Hope, A. D., Pittman, A. M., Lashley, T., Canet-Aviles, R., Miller, D. W., McLendon, C., Strand, C., Leonard, A. J., Abou-Sleiman, P. M., Healy, D. G., Ariga, H., Wood, N. W., de Silva, R., Revesz, T., … Lees, A. J. (2004). The expression of DJ-1 (PARK7) in normal human CNS and idiopathic Parkinson's disease. *Brain*, *127*(2), 420–430. https://doi.org/10.1093/brain/awh054

Bandyopadhyay, S., & Cookson, M. R. (2004). Evolutionary and functional relationships within the DJ1 superfamily. *BMC Evolutionary Biology*, *4*, 6. https://doi.org/10.1186/1471-2148-4-6

Berger, M. T., Hemmler, D., Diederich, P., Rychlik, M., Marshall, J. W., & Schmitt-Kopplin, P. (2022). Open Search of Peptide Glycation Products from Tandem Mass Spectra. *Analytical Chemistry*, *94*(15), 5953–5961. https://doi.org/10.1021/acs.analchem.2c00388

Blauwendraat, C., Nalls, M. A., & Singleton, A. B. (2020). The genetic architecture of Parkinson's disease. *The Lancet. Neurology*, *19*(2), 170–178. https://doi.org/10.1016/S1474-4422(19)30287-X

Bloem, B. R., Okun, M. S., & Klein, C. (2021). Parkinson's disease. *Lancet (London, England)*, *397*(10291), 2284–2303. https://doi.org/10.1016/S0140-6736(21)00218-X

Bolam, J. P., & Pissadaki, E. K. (2012). Living on the edge with too many mouths to feed: Why dopamine neurons die. *Movement Disorders*, *27*(12), 1478–1483. https://doi.org/10.1002/mds.25135

Bonifati, V. (2003). Mutations in the DJ-1 Gene Associated with Autosomal Recessive Early-Onset Parkinsonism. *Science*, *299*(5604), 256–259. https://doi.org/10.1126/science.1077209

Braak, H., Del Tredici, K., Rüb, U., de Vos, R. A. I., Jansen Steur, E. N. H., & Braak, E. (2003). Staging of brain pathology related to sporadic Parkinson's disease. *Neurobiology of Aging*, *24*(2), 197–211. https://doi.org/10.1016/s0197-4580(02)00065-9

Bradford, M. M. (1976). A rapid and sensitive method for the quantitation of microgram quantities of protein utilizing the principle of protein-dye binding. *Analytical Biochemistry*, *72*, 248–254. https://doi.org/10.1006/abio.1976.9999

Camacho-Soto, A., Warden, M. N., Searles Nielsen, S., Salter, A., Brody, D. L., Prather, H., & Racette, B. A. (2017). Traumatic brain injury in the prodromal

period of Parkinson's disease: A large epidemiological study using medicare data. *Annals of Neurology*, *82*(5), 744–754. https://doi.org/10.1002/ana.25074

Canet-Avilés, R. M., Wilson, M. A., Miller, D. W., Ahmad, R., McLendon, C., Bandyopadhyay, S., Baptista, M. J., Ringe, D., Petsko, G. A., & Cookson, M. R. (2004). The Parkinson's disease protein DJ-1 is neuroprotective due to cysteine-sulfinic acid-driven mitochondrial localization. *Proceedings of the National Academy of Sciences of the United States of America*, *101*(24), 9103–9108. https://doi.org/10.1073/pnas.0402959101

Chaudhuri, K. R., & Schapira, A. H. V. (2009). Non-motor symptoms of Parkinson's disease: Dopaminergic pathophysiology and treatment. *The Lancet. Neurology*, *8*(5), 464–474. https://doi.org/10.1016/S1474-4422(09)70068-7

Chen, J., Li, L., & Chin, L.-S. (2010). Parkinson disease protein DJ-1 converts from a zymogen to a protease by carboxyl-terminal cleavage. *Human Molecular Genetics*, *19*(12), 2395–2408. https://doi.org/10.1093/hmg/ddq113

Chen, J.-H., Lin, X., Bu, C., & Zhang, X. (2018). Role of advanced glycation end products in mobility and considerations in possible dietary and nutritional intervention strategies. *Nutrition & Metabolism*, *15*, 72. https://doi.org/10.1186/s12986-018-0306-7

Chiu, C.-Y., Yang, R.-S., Sheu, M.-L., Chan, D.-C., Yang, T.-H., Tsai, K.-S., Chiang, C.-K., & Liu, S.-H. (2016). Advanced glycation end-products induce skeletal muscle atrophy and dysfunction in diabetic mice via a RAGE-mediated, AMPK-down-regulated, Akt pathway. *The Journal of Pathology*, *238*(3), 470–482. https://doi.org/10.1002/path.4674

Choi, J., Sullards, M. C., Olzmann, J. A., Rees, H. D., Weintraub, S. T., Bostwick, D. E., Gearing, M., Levey, A. I., Chin, L.-S., & Li, L. (2006). Oxidative Damage of DJ-1 Is Linked to Sporadic Parkinson and Alzheimer Diseases. *The Journal of*

Biological Chemistry, *281*(16), 10816–10824. https://doi.org/10.1074/jbc.M509079200

Choi, J., Tak, S., Jung, H.-M., Cha, S., Hwang, E., Lee, D., Lee, J.-H., Ryu, K.-S., & Park, C. (2023). Kinetic evidence in favor of glyoxalase III and against deglycase activity of DJ-1. *Protein Science: A Publication of the Protein Society*, *32*(5), e4641. https://doi.org/10.1002/pro.4641

Chong, J., Wishart, D. S., & Xia, J. (2019). Using MetaboAnalyst 4.0 for Comprehensive and Integrative Metabolomics Data Analysis. *Current Protocols in Bioinformatics*, *68*(1), e86. https://doi.org/10.1002/cpbi.86

Clark, L. N., Ross, B. M., Wang, Y., Mejia-Santana, H., Harris, J., Louis, E. D., Cote, L. J., Andrews, H., Fahn, S., Waters, C., Ford, B., Frucht, S., Ottman, R., & Marder, K. (2007). Mutations in the glucocerebrosidase gene are associated with early-onset Parkinson disease. *Neurology*, *69*(12), 1270–1277. https://doi.org/10.1212/01.wnl.0000276989.17578.02

Clements, C. M., McNally, R. S., Conti, B. J., Mak, T. W., & Ting, J. P.-Y. (2006). DJ-1, a cancer- and Parkinson's disease-associated protein, stabilizes the antioxidant transcriptional master regulator Nrf2. *Proceedings of the National Academy of Sciences of the United States of America*, *103*(41), 15091–15096. https://doi.org/10.1073/pnas.0607260103

Damier, P., Hirsch, E. C., Agid, Y., & Graybiel, A. M. (1999). The substantia nigra of the human brain. II. Patterns of loss of dopamine-containing neurons in Parkinson's disease. *Brain: A Journal of Neurology*, *122 (Pt 8)*, 1437–1448. https://doi.org/10.1093/brain/122.8.1437

Dawson, T. M., Ko, H. S., & Dawson, V. L. (2010). Genetic animal models of Parkinson's disease. *Neuron*, *66*(5), 646–661. https://doi.org/10.1016/j.neuron.2010.04.034

de Vos, L. C., Lefrandt, J. D., Dullaart, R. P. F., Zeebregts, C. J., & Smit, A. J. (2016). Advanced glycation end products: An emerging biomarker for adverse outcome in patients with peripheral artery disease. *Atherosclerosis*, *254*, 291–299. https://doi.org/10.1016/j.atherosclerosis.2016.10.012

Delenclos, M., Jones, D. R., McLean, P. J., & Uitti, R. J. (2016). Biomarkers in Parkinson's disease: Advances and strategies. *Parkinsonism & Related Disorders*, *22 Suppl 1*(Suppl 1), S106-110. https://doi.org/10.1016/j.parkreldis.2015.09.048

Dias, V., Junn, E., & Mouradian, M. M. (2013). The role of oxidative stress in Parkinson's disease. *Journal of Parkinson's Disease*, *3*(4), 461–491. https://doi.org/10.3233/JPD-130230

Dijkstra, A. A., Voorn, P., Berendse, H. W., Groenewegen, H. J., Netherlands Brain Bank, Rozemuller, A. J. M., & van de Berg, W. D. J. (2014). Stage-dependent nigral neuronal loss in incidental Lewy body and Parkinson's disease. *Movement Disorders: Official Journal of the Movement Disorder Society*, *29*(10), 1244–1251. https://doi.org/10.1002/mds.25952

Dorsey, E. R., Sherer, T., Okun, M. S., & Bloem, B. R. (2018). The Emerging Evidence of the Parkinson Pandemic. *Journal of Parkinson's Disease*, *8*(s1), S3–S8. https://doi.org/10.3233/JPD-181474

Dos Santos, M., Backer, S., Saintpierre, B., Izac, B., Andrieu, M., Letourneur, F., Relaix, F., Sotiropoulos, A., & Maire, P. (2020). Single-nucleus RNA-seq and FISH identify coordinated transcriptional activity in mammalian myofibers. *Nature Communications*, *11*(1), 5102. https://doi.org/10.1038/s41467-020-18789-8

Fan, J., Ren, H., Jia, N., Fei, E., Zhou, T., Jiang, P., Wu, M., & Wang, G. (2008). DJ-1 decreases Bax expression through repressing p53 transcriptional activity. *The*

Journal of Biological Chemistry, *283*(7), 4022–4030. https://doi.org/10.1074/jbc.M707176200

Fanning, S., Selkoe, D., & Dettmer, U. (2020). Parkinson's disease: Proteinopathy or lipidopathy? *NPJ Parkinson's Disease*, *6*, 3. https://doi.org/10.1038/s41531-019-0103-7

Fearnley, J. M., & Lees, A. J. (1991). Ageing and Parkinson's disease: Substantia nigra regional selectivity. *Brain: A Journal of Neurology*, *114 (Pt 5)*, 2283–2301. https://doi.org/10.1093/brain/114.5.2283

Fu, C., Wu, C., Liu, T., Ago, T., Zhai, P., Sadoshima, J., & Li, H. (2009). Elucidation of Thioredoxin Target Protein Networks in Mouse. *Molecular & Cellular Proteomics : MCP*, *8*(7), 1674–1687. https://doi.org/10.1074/mcp.M800580-MCP200

Gaenslen, A., Swid, I., Liepelt-Scarfone, I., Godau, J., & Berg, D. (2011). The patients' perception of prodromal symptoms before the initial diagnosis of Parkinson's disease. *Movement Disorders: Official Journal of the Movement Disorder Society*, *26*(4), 653–658. https://doi.org/10.1002/mds.23499

Gao, Q., Jacob-Dolan, J. W., & Scheck, R. A. (2023). Parkinsonism-Associated Protein DJ-1 Is an Antagonist, Not an Eraser, for Protein Glycation. *Biochemistry*, *62*(6), 1181–1190. https://doi.org/10.1021/acs.biochem.3c00028

Gatto, L., & Lilley, K. S. (2012). MSnbase-an R/Bioconductor package for isobaric tagged mass spectrometry data visualization, processing and quantitation. *Bioinformatics (Oxford, England)*, *28*(2), 288–289. https://doi.org/10.1093/bioinformatics/btr645

GBD 2016 Neurology Collaborators. (2019). Global, regional, and national burden of neurological disorders, 1990-2016: A systematic analysis for the Global Burden

of Disease Study 2016. *The Lancet. Neurology*, *18*(5), 459–480. https://doi.org/10.1016/S1474-4422(18)30499-X

Girotto, S., Cendron, L., Bisaglia, M., Tessari, I., Mammi, S., Zanotti, G., & Bubacco, L. (2014). DJ-1 is a copper chaperone acting on SOD1 activation. *The Journal of Biological Chemistry*, *289*(15), 10887–10899. https://doi.org/10.1074/jbc.M113.535112

Greifenhagen, U., Frolov, A., Blüher, M., & Hoffmann, R. (2016). Plasma Proteins Modified by Advanced Glycation End Products (AGEs) Reveal Site-specific Susceptibilities to Glycemic Control in Patients with Type 2 Diabetes. *The Journal of Biological Chemistry*, *291*(18), 9610–9616. https://doi.org/10.1074/jbc.M115.702860

Heremans, I. P., Caligiore, F., Gerin, I., Bury, M., Lutz, M., Graff, J., Stroobant, V., Vertommen, D., Teleman, A. A., Van Schaftingen, E., & Bommer, G. T. (2022). Parkinson's disease protein PARK7 prevents metabolite and protein damage caused by a glycolytic metabolite. *Proceedings of the National Academy of Sciences of the United States of America*, *119*(4), e2111338119. https://doi.org/10.1073/pnas.2111338119

Im, J.-Y., Lee, K.-W., Woo, J.-M., Junn, E., & Mouradian, M. M. (2012). DJ-1 induces thioredoxin 1 expression through the Nrf2 pathway. *Human Molecular Genetics*, *21*(13), 3013–3024. https://doi.org/10.1093/hmg/dds131

Imberechts, D., Kinnart, I., Wauters, F., Terbeek, J., Manders, L., Wierda, K., Eggermont, K., Madeiro, R. F., Sue, C., Verfaillie, C., & Vandenberghe, W. (2022). DJ-1 is an essential downstream mediator in PINK1/parkin-dependent mitophagy. *Brain: A Journal of Neurology*, *145*(12), 4368–4384. https://doi.org/10.1093/brain/awac313

Jain, D., Jain, R., Eberhard, D., Eglinger, J., Bugliani, M., Piemonti, L., Marchetti, P., & Lammert, E. (2012). Age- and diet-dependent requirement of DJ-1 for glucose homeostasis in mice with implications for human type 2 diabetes. *Journal of Molecular Cell Biology*, *4*(4), 221–230. https://doi.org/10.1093/jmcb/mjs025

Jain, D., Weber, G., Eberhard, D., Mehana, A. E., Eglinger, J., Welters, A., Bartosinska, B., Jeruschke, K., Weiss, J., Päth, G., Ariga, H., Seufert, J., & Lammert, E. (2015). DJ-1 Protects Pancreatic Beta Cells from Cytokine- and Streptozotocin-Mediated Cell Death. *PLoS ONE*, *10*(9), e0138535. https://doi.org/10.1371/journal.pone.0138535

Kalapos, M. P. (2013). Where does plasma methylglyoxal originate from? *Diabetes Research and Clinical Practice*, *99*(3), 260–271. https://doi.org/10.1016/j.diabres.2012.11.003

Kalia, L. V., & Lang, A. E. (2015). Parkinson's disease. *Lancet (London, England)*, *386*(9996), 896–912. https://doi.org/10.1016/S0140-6736(14)61393-3

Katunina, E. A., Blokhin, V., Nodel, M. R., Pavlova, E. N., Kalinkin, A. L., Kucheryanu, V. G., Alekperova, L., Selikhova, M. V., Martynov, M. Y., & Ugrumov, M. V. (2023). Searching for Biomarkers in the Blood of Patients at Risk of Developing Parkinson's Disease at the Prodromal Stage. *International Journal of Molecular Sciences*, *24*(3), 1842. https://doi.org/10.3390/ijms24031842

Kim, J.-M., Jang, H.-J., Choi, S. Y., Park, S.-A., Kim, I. S., Yang, Y. R., Lee, Y. H., Ryu, S. H., & Suh, P.-G. (2014). DJ-1 contributes to adipogenesis and obesity-induced inflammation. *Scientific Reports*, *4*(1), Article 1. https://doi.org/10.1038/srep04805

Kinumi, T., Kimata, J., Taira, T., Ariga, H., & Niki, E. (2004). Cysteine-106 of DJ-1 is the most sensitive cysteine residue to hydrogen peroxide-mediated oxidation in vivo in human umbilical vein endothelial cells. *Biochemical and Biophysical*

Research Communications, *317*(3), 722–728. https://doi.org/10.1016/j.bbrc.2004.03.110

Knippenberg, S., Sipos, J., Thau-Habermann, N., Körner, S., Rath, K. J., Dengler, R., & Petri, S. (2013). Altered expression of DJ-1 and PINK1 in sporadic ALS and in the SOD1(G93A) ALS mouse model. *Journal of Neuropathology and Experimental Neurology*, *72*(11), 1052–1061. https://doi.org/10.1097/NEN.0000000000000004

Kumaran, R., Kingsbury, A., Coulter, I., Lashley, T., Williams, D., de Silva, R., Mann, D., Revesz, T., Lees, A., & Bandopadhyay, R. (2007). DJ-1 (PARK7) is associated with 3R and 4R tau neuronal and glial inclusions in neurodegenerative disorders. *Neurobiology of Disease*, *28*(1), 122–132. https://doi.org/10.1016/j.nbd.2007.07.012

Lc, de V., Jd, L., Rp, D., Cj, Z., & Aj, S. (2016). Advanced glycation end products: An emerging biomarker for adverse outcome in patients with peripheral artery disease. *Atherosclerosis*, *254*. https://doi.org/10.1016/j.atherosclerosis.2016.10.012

Lee, J., Song, J., Kwon, K., Jang, S., Kim, C., Baek, K., Kim, J., & Park, C. (2012). Human DJ-1 and its homologs are novel glyoxalases. *Human Molecular Genetics*, *21*(14), 3215–3225. https://doi.org/10.1093/hmg/dds155

Lev, N., Barhum, Y., Lotan, I., Steiner, I., & Offen, D. (2015). DJ-1 Knockout Augments Disease Severity and Shortens Survival in a Mouse Model of ALS. *PLoS ONE*, *10*(3), e0117190. https://doi.org/10.1371/journal.pone.0117190

Lind-Holm Mogensen, F., Scafidi, A., Poli, A., & Michelucci, A. (2023). PARK7/DJ-1 in microglia: Implications in Parkinson's disease and relevance as a therapeutic target. *Journal of Neuroinflammation*, *20*(1), 95. https://doi.org/10.1186/s12974-023-02776-z

Lotharius, J., & Brundin, P. (2002). Pathogenesis of Parkinson's disease: Dopamine, vesicles and alpha-synuclein. *Nature Reviews. Neuroscience*, *3*(12), 932–942. https://doi.org/10.1038/nrn983

Lucas, J. I., & Marín, I. (2007). A new evolutionary paradigm for the Parkinson disease gene DJ-1. *Molecular Biology and Evolution*, *24*(2), 551–561. https://doi.org/10.1093/molbev/msl186

Luevano-Contreras, C., & Chapman-Novakofski, K. (2010). Dietary Advanced Glycation End Products and Aging. *Nutrients*, *2*(12), 1247–1265. https://doi.org/10.3390/nu2121247

Mackay, D. F., Russell, E. R., Stewart, K., MacLean, J. A., Pell, J. P., & Stewart, W. (2019). Neurodegenerative Disease Mortality among Former Professional Soccer Players. *The New England Journal of Medicine*, *381*(19), 1801–1808. https://doi.org/10.1056/NEJMoa1908483

Mahlknecht, P., Seppi, K., & Poewe, W. (2015). The Concept of Prodromal Parkinson's Disease. *Journal of Parkinson's Disease*, *5*(4), 681–697. https://doi.org/10.3233/JPD-150685

Makita, Z., Vlassara, H., Rayfield, E., Cartwright, K., Friedman, E., Rodby, R., Cerami, A., & Bucala, R. (1992). Hemoglobin-AGE: A Circulating Marker of Advanced Glycosylation. *Science*, *258*(5082), 651–653. https://doi.org/10.1126/science.1411574

Mazza, M. C., Shuck, S. C., Lin, J., Moxley, M. A., Termini, J., Cookson, M. R., & Wilson, M. A. (2022). DJ-1 is not a deglycase and makes a modest contribution to cellular defense against methylglyoxal damage in neurons. *Journal of Neurochemistry*, *162*(3), 245–261. https://doi.org/10.1111/jnc.15656

McKay, N. D., Robinson, B., Brodie, R., & Rooke-Allen, N. (1983). Glucose transport and metabolism in cultured human skin fibroblasts. *Biochimica Et Biophysica Acta*, *762*(2), 198–204. https://doi.org/10.1016/0167-4889(83)90071-x

McNally, R. S., Davis, B. K., Clements, C. M., Accavitti-Loper, M. A., Mak, T. W., & Ting, J. P.-Y. (2011). DJ-1 Enhances Cell Survival through the Binding of Cezanne, a Negative Regulator of NF-κB. *The Journal of Biological Chemistry*, *286*(6), 4098–4106. https://doi.org/10.1074/jbc.M110.147371

Mencke, P., Boussaad, I., Önal, G., Kievit, A. J. A., Boon, A. J. W., Mandemakers, W., Bonifati, V., & Krüger, R. (2022). Generation and characterization of a genetic Parkinson's disease-patient derived iPSC line DJ-1-delP (LCSBi008-A). *Stem Cell Research*, *62*, 102792. https://doi.org/10.1016/j.scr.2022.102792

Merz, K. E., & Thurmond, D. C. (2020). Role of Skeletal Muscle in Insulin Resistance and Glucose Uptake. *Comprehensive Physiology*, *10*(3), 785–809. https://doi.org/10.1002/cphy.c190029

Meulener, M. C., Xu, K., Thomson, L., Ischiropoulos, H., & Bonini, N. M. (2006). Mutational analysis of DJ-1 in Drosophila implicates functional inactivation by oxidative damage and aging. *Proceedings of the National Academy of Sciences*, *103*(33), 12517–12522. https://doi.org/10.1073/pnas.0601891103

Miyata, T., Ueda, Y., Yoshida, A., Sugiyama, S., Iida, Y., Jadoul, M., Maeda, K., Kurokawa, K., & van Ypersele de Strihou, C. (1997). Clearance of pentosidine, an advanced glycation end product, by different modalities of renal replacement therapy. *Kidney International*, *51*(3), 880–887. https://doi.org/10.1038/ki.1997.124

Monden, M., Koyama, H., Otsuka, Y., Morioka, T., Mori, K., Shoji, T., Mima, Y., Motoyama, K., Fukumoto, S., Shioi, A., Emoto, M., Yamamoto, Y., Yamamoto, H., Nishizawa, Y., Kurajoh, M., Yamamoto, T., & Inaba, M. (2013). Receptor for

Advanced Glycation End Products Regulates Adipocyte Hypertrophy and Insulin Sensitivity in Mice. *Diabetes*, *62*(2), 478–489. https://doi.org/10.2337/db11-1116

Monnier, V. M., & Sell, D. R. (2006). Prevention and repair of protein damage by the Maillard reaction in vivo. *Rejuvenation Research*, *9*(2), 264–273. https://doi.org/10.1089/rej.2006.9.264

Mosharov, E. V., Larsen, K. E., Kanter, E., Phillips, K. A., Wilson, K., Schmitz, Y., Krantz, D. E., Kobayashi, K., Edwards, R. H., & Sulzer, D. (2009). Interplay between Cytosolic Dopamine, Calcium, and α-Synuclein Causes Selective Death of Substantia Nigra Neurons. *Neuron*, *62*(2), 218–229. https://doi.org/10.1016/j.neuron.2009.01.033

Münch, G., Lüth, H. J., Wong, A., Arendt, T., Hirsch, E., Ravid, R., & Riederer, P. (2000). Crosslinking of alpha-synuclein by advanced glycation endproducts—An early pathophysiological step in Lewy body formation? *Journal of Chemical Neuroanatomy*, *20*(3–4), 253–257. https://doi.org/10.1016/s0891-0618(00)00096-x

Muschet, C., Möller, G., Prehn, C., de Angelis, M. H., Adamski, J., & Tokarz, J. (2016). Removing the bottlenecks of cell culture metabolomics: Fast normalization procedure, correlation of metabolites to cell number, and impact of the cell harvesting method. *Metabolomics*, *12*(10), 151. https://doi.org/10.1007/s11306-016-1104-8

Nagakubo, D., Taira, T., Kitaura, H., Ikeda, M., Tamai, K., Iguchi-Ariga, S. M., & Ariga, H. (1997). DJ-1, a novel oncogene which transforms mouse NIH3T3 cells in cooperation with ras. *Biochemical and Biophysical Research Communications*, *231*(2), 509–513. https://doi.org/10.1006/bbrc.1997.6132

Narendra, D. P., Isonaka, R., Nguyen, D., Schindler, A. B., Kokkinis, A. D., Ehrlich, D., Bardakjian, T. M., Goldstein, D. S., Liang, T.-W., & Gonzalez-Alegre, P. (2019). Peripheral synucleinopathy in a DJ1 patient with Parkinson disease, cataracts, and hearing loss. *Neurology*, *92*(23), 1113–1115. https://doi.org/10.1212/WNL.0000000000007614

Neumann, M., Müller, V., Görner, K., Kretzschmar, H. A., Haass, C., & Kahle, P. J. (2004). Pathological properties of the Parkinson's disease-associated protein DJ-1 in alpha-synucleinopathies and tauopathies: Relevance for multiple system atrophy and Pick's disease. *Acta Neuropathologica*, *107*(6), 489–496. https://doi.org/10.1007/s00401-004-0834-2

Nichols, W. C., Pankratz, N., Marek, D. K., Pauciulo, M. W., Elsaesser, V. E., Halter, C. A., Rudolph, A., Wojcieszek, J., Pfeiffer, R. F., Foroud, T., & Parkinson Study Group-PROGENI Investigators. (2009). Mutations in GBA are associated with familial Parkinson disease susceptibility and age at onset. *Neurology*, *72*(4), 310–316. https://doi.org/10.1212/01.wnl.0000327823.81237.d1

Noyce, A. J., Bestwick, J. P., Silveira-Moriyama, L., Hawkes, C. H., Giovannoni, G., Lees, A. J., & Schrag, A. (2012). Meta-Analysis of Early Nonmotor Features and Risk Factors for Parkinson Disease. *Annals of Neurology*, *72*(6), 893–901. https://doi.org/10.1002/ana.23687

Pamplona, R., Ilieva, E., Ayala, V., Bellmunt, M. J., Cacabelos, D., Dalfo, E., Ferrer, I., & Portero-Otin, M. (2008). Maillard reaction versus other nonenzymatic modifications in neurodegenerative processes. *Annals of the New York Academy of Sciences*, *1126*, 315–319. https://doi.org/10.1196/annals.1433.014

Perry, V. H. (2004). The influence of systemic inflammation on inflammation in the brain: Implications for chronic neurodegenerative disease. *Brain, Behavior, and Immunity*, *18*(5), 407–413. https://doi.org/10.1016/j.bbi.2004.01.004

Pfaff, D. H., Fleming, T., Nawroth, P., & Teleman, A. A. (2017a). Evidence Against a Role for the Parkinsonism-associated Protein DJ-1 in Methylglyoxal Detoxification*. *Journal of Biological Chemistry*, *292*(2), 685–690. https://doi.org/10.1074/jbc.M116.743823

Pfaff, D. H., Fleming, T., Nawroth, P., & Teleman, A. A. (2017b). Reply to Richarme: Evidence against a role of DJ-1 in methylglyoxal detoxification. *The Journal of Biological Chemistry*, *292*(31), 12784–12785. https://doi.org/10.1074/jbc.L117.798579

Pham, T. T., Giesert, F., Röthig, A., Floss, T., Kallnik, M., Weindl, K., Hölter, S. M., Ahting, U., Prokisch, H., Becker, L., Klopstock, T., Angelis, M. H. de, Beyer, K., Görner, K., Kahle, P. J., Weisenhorn, D. M. V., & Wurst, W. (2010). DJ-1-deficient mice show less TH-positive neurons in the ventral tegmental area and exhibit non-motoric behavioural impairments. *Genes, Brain and Behavior*, *9*(3), 305–317. https://doi.org/10.1111/j.1601-183X.2009.00559.x

Pinter, B., Diem-Zangerl, A., Wenning, G. K., Scherfler, C., Oberaigner, W., Seppi, K., & Poewe, W. (2015). Mortality in Parkinson's disease: A 38-year follow-up study. *Movement Disorders*, *30*(2), 266–269. https://doi.org/10.1002/mds.26060

Pissadaki, E. K., & Bolam, J. P. (2013). The energy cost of action potential propagation in dopamine neurons: Clues to susceptibility in Parkinson's disease. *Frontiers in Computational Neuroscience*, *7*, 13. https://doi.org/10.3389/fncom.2013.00013

Poewe, W., Seppi, K., Tanner, C. M., Halliday, G. M., Brundin, P., Volkmann, J., Schrag, A.-E., & Lang, A. E. (2017). Parkinson disease. *Nature Reviews Disease Primers*, *3*(1), 17013. https://doi.org/10.1038/nrdp.2017.13

Postuma, R. B., Berg, D., Stern, M., Poewe, W., Olanow, C. W., Oertel, W., Obeso, J., Marek, K., Litvan, I., Lang, A. E., Halliday, G., Goetz, C. G., Gasser, T., Dubois, B., Chan, P., Bloem, B. R., Adler, C. H., & Deuschl, G. (2015). MDS clinical diagnostic criteria for Parkinson's disease. *Movement Disorders*, *30*(12), 1591–1601. https://doi.org/10.1002/mds.26424

Pringsheim, T., Jette, N., Frolkis, A., & Steeves, T. D. L. (2014). The prevalence of Parkinson's disease: A systematic review and meta-analysis. *Movement Disorders: Official Journal of the Movement Disorder Society*, *29*(13), 1583–1590. https://doi.org/10.1002/mds.25945

Rabbani, N., Ashour, A., & Thornalley, P. J. (2016). Mass spectrometric determination of early and advanced glycation in biology. *Glycoconjugate Journal*, *33*(4), 553–568. https://doi.org/10.1007/s10719-016-9709-8

Rabbani, N., & Thornalley, P. J. (2012). Glycation research in amino acids: A place to call home. *Amino Acids*, *42*(4), 1087–1096. https://doi.org/10.1007/s00726-010-0782-1

Raninga, P. V., Trapani, G. D., & Tonissen, K. F. (2014). Cross Talk between Two Antioxidant Systems, Thioredoxin and DJ-1: Consequences for Cancer. *Oncoscience*, *1*(1), 95–110.

Richarme, G. (2017). Response to manuscript by Pfaff et al.: Evidence against a role of DJ-1 in methylglyoxal detoxification. *The Journal of Biological Chemistry*, *292*(31), 12783. https://doi.org/10.1074/jbc.L117.797464

Richarme, G., Abdallah, J., Mathas, N., Gautier, V., & Dairou, J. (2018). Further characterization of the Maillard deglycase DJ-1 and its prokaryotic homologs, deglycase 1/Hsp31, deglycase 2/YhbO, and deglycase 3/YajL. *Biochemical and Biophysical Research Communications*, *503*(2), 703–709. https://doi.org/10.1016/j.bbrc.2018.06.064

Richarme, G., & Dairou, J. (2017). Parkinsonism-associated protein DJ-1 is a bona fide deglycase. *Biochemical and Biophysical Research Communications*, *483*(1), 387–391. https://doi.org/10.1016/j.bbrc.2016.12.134

Richarme, G., Mihoub, M., Dairou, J., Bui, L. C., Leger, T., & Lamouri, A. (2015). Parkinsonism-associated protein DJ-1/Park7 is a major protein deglycase that repairs methylglyoxal- and glyoxal-glycated cysteine, arginine, and lysine residues. *The Journal of Biological Chemistry*, *290*(3), 1885–1897. https://doi.org/10.1074/jbc.M114.597815

Rizzu, P., Hinkle, D. A., Zhukareva, V., Bonifati, V., Severijnen, L.-A., Martinez, D., Ravid, R., Kamphorst, W., Eberwine, J. H., Lee, V. M.-Y., Trojanowski, J. Q., & Heutink, P. (2004). DJ-1 colocalizes with tau inclusions: A link between parkinsonism and dementia. *Annals of Neurology*, *55*(1), 113–118. https://doi.org/10.1002/ana.10782

Rossi, A., Berger, K., Chen, H., Leslie, D., Mailman, R. B., & Huang, X. (2018). Projection of the prevalence of Parkinson's disease in the coming decades: Revisited. *Movement Disorders: Official Journal of the Movement Disorder Society*, *33*(1), 156–159. https://doi.org/10.1002/mds.27063

Ruiz-Lopez, M., Freitas, M. E., Oliveira, L. M., Munhoz, R. P., Fox, S. H., Rohani, M., Rogaeva, E., Lang, A. E., & Fasano, A. (2019). Diagnostic delay in Parkinson's disease caused by PRKN mutations. *Parkinsonism & Related Disorders*, *63*, 217–220. https://doi.org/10.1016/j.parkreldis.2019.01.010

Sajjad, M. U., Green, E. W., Miller-Fleming, L., Hands, S., Herrera, F., Campesan, S., Khoshnan, A., Outeiro, T. F., Giorgini, F., & Wyttenbach, A. (2014). DJ-1 modulates aggregation and pathogenesis in models of Huntington's disease. *Human Molecular Genetics*, *23*(3), 755–766. https://doi.org/10.1093/hmg/ddt466

Salahuddin, P., Rabbani, G., & Khan, R. H. (2014). The role of advanced glycation end products in various types of neurodegenerative disease: A therapeutic approach. *Cellular & Molecular Biology Letters*, *19*(3), 407–437. https://doi.org/10.2478/s11658-014-0205-5

Samuel, V. T., Petersen, K. F., & Shulman, G. I. (2010). Lipid-induced insulin resistance: Unravelling the mechanism. *Lancet (London, England)*, *375*(9733), 2267–2277. https://doi.org/10.1016/S0140-6736(10)60408-4

Savica, R., Grossardt, B. R., Bower, J. H., Ahlskog, J. E., & Rocca, W. A. (2013). Incidence and pathology of synucleinopathies and tauopathies related to parkinsonism. *JAMA Neurology*, *70*(7), 859–866. https://doi.org/10.1001/jamaneurol.2013.114

Schaum, N., Lehallier, B., Hahn, O., Pálovics, R., Hosseinzadeh, S., Lee, S. E., Sit, R., Lee, D. P., Losada, P. M., Zardeneta, M. E., Fehlmann, T., Webber, J. T., McGeever, A., Calcuttawala, K., Zhang, H., Berdnik, D., Mathur, V., Tan, W., Zee, A., … Wyss-Coray, T. (2020). Ageing hallmarks exhibit organ-specific temporal signatures. *Nature*, *583*(7817), 596–602. https://doi.org/10.1038/s41586-020-2499-y

Schiaffino, S., Gorza, L., Sartore, S., Saggin, L., Ausoni, S., Vianello, M., Gundersen, K., & Lømo, T. (1989). Three myosin heavy chain isoforms in type 2 skeletal muscle fibres. *Journal of Muscle Research and Cell Motility*, *10*(3), 197–205. https://doi.org/10.1007/BF01739810

Schiaffino, S., & Reggiani, C. (2011). Fiber types in mammalian skeletal muscles. *Physiological Reviews*, *91*(4), 1447–1531. https://doi.org/10.1152/physrev.00031.2010

Schmidt, S., Vogt Weisenhorn, D. M., & Wurst, W. (2022). Chapter 5 – “Parkinson’s disease – A role of non-enzymatic posttranslational modifications in disease

onset and progression?" *Molecular Aspects of Medicine*, *86*, 101096. https://doi.org/10.1016/j.mam.2022.101096

Schmidt, T., Samaras, P., Frejno, M., Gessulat, S., Barnert, M., Kienegger, H., Krcmar, H., Schlegl, J., Ehrlich, H.-C., Aiche, S., Kuster, B., & Wilhelm, M. (2018). ProteomicsDB. *Nucleic Acids Research*, *46*(D1), D1271–D1281. https://doi.org/10.1093/nar/gkx1029

Sebeková, K., Kupcová, V., Schinzel, R., & Heidland, A. (2002). Markedly elevated levels of plasma advanced glycation end products in patients with liver cirrhosis—Amelioration by liver transplantation. *Journal of Hepatology*, *36*(1), 66–71. https://doi.org/10.1016/s0168-8278(01)00232-x

Seyfarth, K., Poschmann, G., Rozman, J., Fromme, T., Rink, N., Hofmann, A., Wurst, W., Stühler, K., & Klingenspor, M. (2015). The development of diet-induced obesity and associated metabolic impairments in Dj-1 deficient mice. *The Journal of Nutritional Biochemistry*, *26*(1), 75–81. https://doi.org/10.1016/j.jnutbio.2014.09.002

Sharma, A., Weber, D., Raupbach, J., Dakal, T. C., Fließbach, K., Ramirez, A., Grune, T., & Wüllner, U. (2020). Advanced glycation end products and protein carbonyl levels in plasma reveal sex-specific differences in Parkinson's and Alzheimer's disease. *Redox Biology*, *34*, 101546. https://doi.org/10.1016/j.redox.2020.101546

Sharma, N., Rao, S. P., & Kalivendi, S. V. (2019). The deglycase activity of DJ-1 mitigates α-synuclein glycation and aggregation in dopaminergic cells: Role of oxidative stress mediated downregulation of DJ-1 in Parkinson's disease. *Free Radical Biology & Medicine*, *135*, 28–37. https://doi.org/10.1016/j.freeradbiomed.2019.02.014

Shendelman, S., Jonason, A., Martinat, C., Leete, T., & Abeliovich, A. (2004). DJ-1 is a redox-dependent molecular chaperone that inhibits alpha-synuclein aggregate formation. *PLoS Biology*, *2*(11), e362. https://doi.org/10.1371/journal.pbio.0020362

Shi, S. Y., Lu, S.-Y., Sivasubramaniyam, T., Revelo, X. S., Cai, E. P., Luk, C. T., Schroer, S. A., Patel, P., Kim, R. H., Bombardier, E., Quadrilatero, J., Tupling, A. R., Mak, T. W., Winer, D. A., & Woo, M. (2015). DJ-1 links muscle ROS production with metabolic reprogramming and systemic energy homeostasis in mice. *Nature Communications*, *6*(1), Article 1. https://doi.org/10.1038/ncomms8415

Shulman, G. I. (2014). Ectopic fat in insulin resistance, dyslipidemia, and cardiometabolic disease. *The New England Journal of Medicine*, *371*(12), 1131–1141. https://doi.org/10.1056/NEJMra1011035

Smith, J. A. B., Murach, K. A., Dyar, K. A., & Zierath, J. R. (2023). Exercise metabolism and adaptation in skeletal muscle. *Nature Reviews. Molecular Cell Biology*, *24*(9), 607–632. https://doi.org/10.1038/s41580-023-00606-x

Solomon, V., Lecker, S. H., & Goldberg, A. L. (1998). The N-end rule pathway catalyzes a major fraction of the protein degradation in skeletal muscle. *The Journal of Biological Chemistry*, *273*(39), 25216–25222. https://doi.org/10.1074/jbc.273.39.25216

Song, F., Hurtado del Pozo, C., Rosario, R., Zou, Y. S., Ananthakrishnan, R., Xu, X., Patel, P. R., Benoit, V. M., Yan, S. F., Li, H., Friedman, R. A., Kim, J. K., Ramasamy, R., Ferrante, A. W., & Schmidt, A. M. (2014). RAGE Regulates the Metabolic and Inflammatory Response to High-Fat Feeding in Mice. *Diabetes*, *63*(6), 1948–1965. https://doi.org/10.2337/db13-1636

Stark, R., & Roden, M. (2007). ESCI Award 2006. Mitochondrial function and endocrine diseases. *European Journal of Clinical Investigation*, *37*(4), 236–248. https://doi.org/10.1111/j.1365-2362.2007.01773.x

Stevens, A. (1998). The contribution of glycation to cataract formation in diabetes. *Journal of the American Optometric Association*, *69*(8), 519–530.

Sun, K., Kusminski, C. M., & Scherer, P. E. (2011). Adipose tissue remodeling and obesity. *The Journal of Clinical Investigation*, *121*(6), 2094–2101. https://doi.org/10.1172/JCI45887

Tabula Muris Consortium, Overall coordination, Logistical coordination, Organ collection and processing, Library preparation and sequencing, Computational data analysis, Cell type annotation, Writing group, Supplemental text writing group, & Principal investigators. (2018). Single-cell transcriptomics of 20 mouse organs creates a Tabula Muris. *Nature*, *562*(7727), 367–372. https://doi.org/10.1038/s41586-018-0590-4

Taipa, R., Pereira, C., Reis, I., Alonso, I., Bastos-Lima, A., Melo-Pires, M., & Magalhães, M. (2016). DJ-1 linked parkinsonism (PARK7) is associated with Lewy body pathology. *Brain: A Journal of Neurology*, *139*(Pt 6), 1680–1687. https://doi.org/10.1093/brain/aww080

Taira, T., Saito, Y., Niki, T., Iguchi-Ariga, S. M. M., Takahashi, K., & Ariga, H. (2004). DJ-1 has a role in antioxidative stress to prevent cell death. *EMBO Reports*, *5*(2), 213–218. https://doi.org/10.1038/sj.embor.7400074

Thornalley, P. J., Langborg, A., & Minhas, H. S. (1999). Formation of glyoxal, methylglyoxal and 3-deoxyglucosone in the glycation of proteins by glucose. *The Biochemical Journal*, *344 Pt 1*(Pt 1), 109–116.

Tiganis, T. (2011). Reactive oxygen species and insulin resistance: The good, the bad and the ugly. *Trends in Pharmacological Sciences*, *32*(2), 82–89. https://doi.org/10.1016/j.tips.2010.11.006

Tokarz, J., Lintelmann, J., Möller, G., & Adamski, J. (2020). Substrate multispecificity among 20β-hydroxysteroid dehydrogenase type 2 members. *Molecular and Cellular Endocrinology*, *510*, 110822. https://doi.org/10.1016/j.mce.2020.110822

Tolosa, E., Wenning, G., & Poewe, W. (2006). The diagnosis of Parkinson's disease. *The Lancet. Neurology*, *5*(1), 75–86. https://doi.org/10.1016/S1474-4422(05)70285-4

Twelves, D., Perkins, K. S. M., & Counsell, C. (2003). Systematic review of incidence studies of Parkinson's disease. *Movement Disorders: Official Journal of the Movement Disorder Society*, *18*(1), 19–31. https://doi.org/10.1002/mds.10305

Van Den Eeden, S. K., Tanner, C. M., Bernstein, A. L., Fross, R. D., Leimpeter, A., Bloch, D. A., & Nelson, L. M. (2003). Incidence of Parkinson's disease: Variation by age, gender, and race/ethnicity. *American Journal of Epidemiology*, *157*(11), 1015–1022. https://doi.org/10.1093/aje/kwg068

Vander Jagt, D. L., & Hunsaker, L. A. (2003). Methylglyoxal metabolism and diabetic complications: Roles of aldose reductase, glyoxalase-I, betaine aldehyde dehydrogenase and 2-oxoaldehyde dehydrogenase. *Chemico-Biological Interactions*, *143–144*, 341–351. https://doi.org/10.1016/s0009-2797(02)00212-0

Varshavsky, A. (2011). The N-end rule pathway and regulation by proteolysis. *Protein Science : A Publication of the Protein Society*, *20*(8), 1298–1345. https://doi.org/10.1002/pro.666

Vicente Miranda, H., & Outeiro, T. F. (2010). The sour side of neurodegenerative disorders: The effects of protein glycation. *The Journal of Pathology*, *221*(1), 13–25. https://doi.org/10.1002/path.2682

Vicente Miranda, H., Szego, É. M., Oliveira, L. M. A., Breda, C., Darendelioglu, E., de Oliveira, R. M., Ferreira, D. G., Gomes, M. A., Rott, R., Oliveira, M., Munari, F., Enguita, F. J., Simões, T., Rodrigues, E. F., Heinrich, M., Martins, I. C., Zamolo, I., Riess, O., Cordeiro, C., … Outeiro, T. F. (2017). Glycation potentiates α-synuclein-associated neurodegeneration in synucleinopathies. *Brain: A Journal of Neurology*, *140*(5), 1399–1419. https://doi.org/10.1093/brain/awx056

Vijiaratnam, N., Simuni, T., Bandmann, O., Morris, H. R., & Foltynie, T. (2021). Progress towards therapies for disease modification in Parkinson's disease. *The Lancet Neurology*, *20*(7), 559–572. https://doi.org/10.1016/S1474-4422(21)00061-2

Wang, Z., Liu, J., Chen, S., Wang, Y., Cao, L., Zhang, Y., Kang, W., Li, H., Gui, Y., Chen, S., & Ding, J. (2011). DJ-1 modulates the expression of Cu/Zn-superoxide dismutase-1 through the Erk1/2-Elk1 pathway in neuroprotection. *Annals of Neurology*, *70*(4), 591–599. https://doi.org/10.1002/ana.22514

Yabuuchi, J., Ueda, S., Yamagishi, S., Nohara, N., Nagasawa, H., Wakabayashi, K., Matsui, T., Yuichiro, H., Kadoguchi, T., Otsuka, T., Gohda, T., & Suzuki, Y. (2020). Association of advanced glycation end products with sarcopenia and frailty in chronic kidney disease. *Scientific Reports*, *10*, 17647. https://doi.org/10.1038/s41598-020-74673-x

Yagmur, E., Tacke, F., Weiss, C., Lahme, B., Manns, M. P., Kiefer, P., Trautwein, C., & Gressner, A. M. (2006). Elevation of Nepsilon-(carboxymethyl)lysine-modified advanced glycation end products in chronic liver disease is an indicator of liver

cirrhosis. *Clinical Biochemistry*, *39*(1), 39–45. https://doi.org/10.1016/j.clinbiochem.2005.07.016

Yanagisawa, D., Kitamura, Y., Inden, M., Takata, K., Taniguchi, T., Morikawa, S., Morita, M., Inubushi, T., Tooyama, I., Taira, T., Iguchi-Ariga, S. M., Akaike, A., & Ariga, H. (2008). DJ-1 Protects against Neurodegeneration Caused by Focal Cerebral Ischemia and Reperfusion in Rats. *Journal of Cerebral Blood Flow & Metabolism*, *28*(3), 563–578. https://doi.org/10.1038/sj.jcbfm.9600553

Yoo, Y. D., Mun, S. R., Ji, C. H., Sung, K. W., Kang, K. Y., Heo, A. J., Lee, S. H., An, J. Y., Hwang, J., Xie, X.-Q., Ciechanover, A., Kim, B. Y., & Kwon, Y. T. (2018). N-terminal arginylation generates a bimodal degron that modulates autophagic proteolysis. *Proceedings of the National Academy of Sciences of the United States of America*, *115*(12), E2716–E2724. https://doi.org/10.1073/pnas.1719110115

Zhou, W., & Freed, C. R. (2005). DJ-1 up-regulates glutathione synthesis during oxidative stress and inhibits A53T alpha-synuclein toxicity. *The Journal of Biological Chemistry*, *280*(52), 43150–43158. https://doi.org/10.1074/jbc.M507124200

Zhou, W., Zhu, M., Wilson, M. A., Petsko, G. A., & Fink, A. L. (2006). The oxidation state of DJ-1 regulates its chaperone activity toward alpha-synuclein. *Journal of Molecular Biology*, *356*(4), 1036–1048. https://doi.org/10.1016/j.jmb.2005.12.030

Zhou, Z. D., Yi, L. X., Wang, D. Q., Lim, T. M., & Tan, E. K. (2023). Role of dopamine in the pathophysiology of Parkinson's disease. *Translational Neurodegeneration*, *12*(1), 44. https://doi.org/10.1186/s40035-023-00378-6

Zondler, L., Miller-Fleming, L., Repici, M., Gonçalves, S., Tenreiro, S., Rosado-Ramos, R., Betzer, C., Straatman, K. R., Jensen, P. H., Giorgini, F., & Outeiro, T. F.

(2014). DJ-1 interactions with α-synuclein attenuate aggregation and cellular toxicity in models of Parkinson's disease. *Cell Death & Disease*, *5*(7), e1350. https://doi.org/10.1038/cddis.2014.307

INDEX OF FIGURES

INDEX OF ABBREVIATIONS

α-GK	α-glycerinyllysine
α-GR	α-glycerinylarginine
α-GTMK	α-glycerinyltrimethyllysine
α-syn	α-synuclein
AD	Alzheimer's disease
AGE	Advanced glycation end product
ALS	Amyotrophic lateral sclerosis
AMPK	AMP-activated protein kinase
ASK1	apoptosis signal-regulating kinase 1
ATG	Start codon
ATP	Adenosine triphosphate
BSA	Bovine serum albumin
BW	Bodyweight
CML	Carboxymethyllysine
CSA	Cross sectional area
DBS	Deep brain stimulation
DIO	Diet-induced obesity
DLB	Dementia Lewy bodies
DMEM	Dulbecco's Modified Eagle Medium
DNA	Deoxyribonucleic acid
echoMRI/NMR	Nuclear magnetic resonance
EDL	Extensor digitorum longus
EE/MR	Energy expenditure/Metabolic rate
eWAT	epididymal white adipose tissue
FBS	Fetal bovine serum
GBA1	Glucosylceramidase beta 1
GO	Glyoxal
GSH	Glutathione
GSH	Gluthatione
HFD	high-fat diet
HFHS	high-fat high-sucrose diet

HILIC-tandem MS/MS	Hydrophilic interaction liquid chromatohraphy-tandem mass spectrometry
IBAQ	Intensity based absolute quantification
K	lysine
KO	knockout
L-DOPA	levodopa
LC	Liquid chromatography
LRRK2	Leucine-rich repeat kinase 2
MetS	Metabolic Syndrome
MGO	Methylglyoxal
MS	Mass spectrometry
MSA	Multiple muscle atrophy
Myh	Myosin heavy chain
NF-kB	Nuclear Factor kappaB
p53	Tumor protein p53
Park7	Parkinsonism associated deglycase
PCA	Principal component analysis
PD	Parkinson's disease
PINK1	PTEN-induced putative kinase 1
PRAK	p38-regulated/activated protein kinase
PRKN	Parkin RBR E3 ubiquitin-protein ligase
PTM	post translational modification
R	Arginine
RAGE	Receptor for Advanced glycation end products
RER/RQ	Respiratory exchange ratio/Respiratoy quotient
RNA	Ribonucleic acid
ROS	Reactive oxygen species
RP-UHPLC-MS/MS	Reversed phase-ultrahigh-performance liquid chromatography-tandem mass spectrometry
SAM	S-adenosylmethionine
SD	Standard deviation
SEM	Standard error of the mean
SN	Substantia nigra
SNpc	Substantia nigra pars compacta

SOD1	superoxide dismutade
T2DM	Type 2 diabetes mellitus
TAA	Stop codon
TMK	Trimethyllysine
TPM	Transcripts per million
Trx	Thioredoxin
UCH-L1	ubiquitin carboxy-terminal hydrolase L1
WT	Wildtype

DECLARATION OF AUTHOR CONTRIBUTIONS

Natalia Prudente de Mello, Michelle Tamara Berger, Kim A Lagerborg, Susanne Keipert, Yingfei Yan, Leopold Weidner, Janina Tokarz, Gabriele Möller, Stefano Ciciliot, Yiming Cheng, Margarita Chudenkova, Anna Artati, Daniela Vogt Weisenhorn, Wolfgang Wurst, Jerzy Adamski, Jennifer Wettmarshausen, Roland Nilsson, Antonella Spinazzola, Diego Perez Rodriguez, Matthew Gegg, Anthony H V Schapira, Giovanni Cossu, Agnita Boon, Anneke Kievit, Wim Mandemakers, Vincenzo Bonifati, Mohit Jain, Martin Jastroch, Philippe Schmitt-Kopplin, Fabiana Perocchi, and Kenneth Allen Dyar

Conceptualization: FP and KAD

Investigation: NPdM, SK, JT, GM, SC, MC, JW, DPR, MG, and KAD

Formal Analysis: NPdM, MTB, KAL, SK, YY, LW, JT, GM, SC, YC, AA, and KAD

Data Curation: NPdM, MTB, KAL, SK, YY, LW, JT, and KAD

Visualization: NPdM, MTB, SK, YY, LW, JT, GM, SC, YC, and KAD

Supervision and Funding Acquisition: FP, and KAD

My contribution to this thesis in detail:

For this thesis, I analyzed the data and interpreted the experimental results, generating the shown figures from the *in vivo* indirect calorimetry and metabolic phenotyping experiments, including bodyweight, total fat mass and fat free mass investigated by nuclear magnetic resonance (EchoMRI), as well as food intake, locomotor activity, energy expenditure, and respiratory exchange ratio (RER) monitored on a TSE system. I analyzed and visualized the fiber size data from the immunofluorescence experiment performed on mouse skeletal muscle. I performed the *in vitro* experiments with fibroblasts cell culture of Park7-related early onset Parkinson's disease, as well as harvested the samples for metabolomics analysis. Additionally, I interpreted the data, participated in the discussions and the design of experimental plans, and wrote this thesis and part of an article manuscript soon to be submitted.

Munich, _____
Natalia Prudente de Mello

Munich, _____
Prof Dr Fabiana Perocchi

PUBLICATIONS

de Mello, NP.[#], Fecher, C.[#], Pastor, AM., Perocchi, F., Misgeld, T. (2023) Ex vivo immunocapture and functional characterization of cell-type-specific mitochondria using MitoTag mice. Nature Protocol 18(7):2181-2220. doi: 10.1038/s41596-023-00831-w. (# equal contribution)

Tai, YH., Engels, D., Locatelli, G., Emmanouilidis, L., Fecher, C., Theodorou, D., Müller, AS., Licht-Mayer, S., Kreutzfeldt, M., Wagner, I., **de Mello, NP.**, Gkotzamani, SN., Trovo, L., Kendirli, A., Aljovic, A., Breckwoldt, MO., Naumann, R., Bareyre, FM., Perocchi, F., Mahad, D., Merkler, D., Lichtenthaler, SF., Kerschensteiner, M., Misgeld, T. (2023) Targeting the TCA cycle can ameliorate widespread axonal energy deficiency in neuroinflammatory lesions. Nature Metabolism **5**, 1364–1381. https://doi.org/10.1038/s42255-023-00838-3

de Mello, NP., Andreotti, DZ., Orellana, AM., Scavone, C., Kawamoto, EM. (2020) Inverse sex-based expression profiles of PTEN and Klotho in mice. Scientific Report. https://doi: 10.1038/s41598-020-77217-5.

Mello, NP.[#]; Orellana, A.M.[#]; Mazucanti, C.H[#]; Morais Lima, G; Scavone, C.; Kawamoto, E.M. (2019) Insulin and Autophagy in Neurodegeneration. Review. Frontiers in Neuroscience. https://doi:10.3389/fnins.2019.00491. (# equal contribution)

Cabral-Costa, J.V.; Andreotti, D.Z.; **Mello, N.P.**; Scavone, C.; Camandola, S.; Kawamoto, E.M. (2018) Intermittent fasting uncovers and rescues cognitive phenotypes in PTEN neuronal haploinsufficient mice. Scientific Reports, v.8, p.8595. https://doi.org/10.1038/s41598-018-26814-6

(NON-PEER-REVIEWED)

Systematic mapping of MCU-mediated mitochondrial calcium signaling networks. De la Herran HD., Vecellio Reane D., Cheng Y., Katona M., Hosp F., Greotti E., Wettmarshausen J., Patron M., Mohr H., **de Mello NP.**, Chudenkova M., Gorza M., Walia S., Feng M.S-F., Leimpek A., Mielenz D., Pellegata N., Langer T., Hajnoczky G., Mann M., Murgia M., Perocchi F. bioRxiv. Preprint posted February 21, 2024. https://doi.org/10.1101/2024.02.20.581153.

ACKNOWLEDGEMENTS

I would like to express my deepest appreciation to my family and partner for their unwavering love, support, and understanding. Their encouragement and belief in me sustained me through the ups and downs of this journey.

I am grateful to my colleagues and friends for their encouragement, discussions, and moral support throughout this endeavor. Their camaraderie and shared experiences made the challenges more manageable and the successes more meaningful.

I am thankful for my supervisor, Prof Dr Fabiana Perocchi, for the opportunity, and all her support, guidance, and mentorship throughout this journey. I am also thankful for Dr Kenneth Dyar for all the experimental support and guidance in the project with his skeletal muscle expertise, and all the collaborators that contributed to this project.

Lastly, I am grateful for all the scientific moments that I experienced during my time in the Institute for Diabetes and Obesity at the Helmholtz Zentrum Munich and at the Graduate School of Systemic Neurosciences.

SPRINGER NATURE LICENSE TERMS AND CONDITIONS

May 16, 2024

This Agreement between Helmholtz Zentrum München -- Natalia Prudente de Mello ("You") and Springer Nature ("Springer Nature") consists of your license details and the terms and conditions provided by Springer Nature and Copyright Clearance Center.

License Number	5790690035647
License date	May 16, 2024
Licensed Content Publisher	Springer Nature
Licensed Content Publication	Nature Reviews Disease Primers
Licensed Content Title	Parkinson disease
Licensed Content Author	Werner Poewe et al
Licensed Content Date	Mar 23, 2017
Type of Use	Thesis/Dissertation
Requestor type	academic/university or research institute
Format	print and electronic
Portion	figures/tables/illustrations
Number of figures/tables/illustrations	1
Would you like a high resolution image with your order?	no
Will you be translating?	no
Circulation/distribution	1 - 29
Author of this Springer Nature content	no
Title of new work	Loss of DJ-1 protein leads to tissue specific accumulation of advanced glycation end products
Institution name	Ludwig-Maximilians-Universität München
Expected presentation	May 2024

date	
Portions	Figure 5
Requestor Location	Helmholtz Zentrum München Ingolstädter Landstraße 1 Neuherberg, 85764 Germany Attn: Helmholtz Zentrum München
Total	**0.00 EUR**
Terms and Conditions	

Advanced glycation end products: An emerging biomarker for adverse outcome in patients with peripheral artery disease

Author: Lisanne C. de Vos,Joop D. Lefrandt,Robin P.F. Dullaart,Clark J. Zeebregts,Andries J. Smit

Publication: Atherosclerosis

Publisher: Elsevier

Date: November 2016

Creative Commons